

1 Evaluating the dendroclimatological potential of blue intensity on 2 multiple conifer species from Tasmania and New Zealand

3 Rob Wilson^{1,4}, Kathy Allen², Patrick Baker², Gretel Boswijk³, Brendan Buckley⁴, Edward Cook⁴,
4 Rosanne D'Arrigo⁴, Dan Druckenbrod⁵, Anthony Fowler³, Margaux Grandjean¹, Paul Krusic⁶, Jonathan
5 Palmer⁷

6 ¹ School of Earth & Environmental Sciences, University of St. Andrews, UK

7 ² School of Ecosystem and Forest Sciences, University of Melbourne, 500 Yarra Boulevard, Richmond 3121, Australia

8 ³ Tree-Ring Laboratory, School of Environment, The University of Auckland, Private Bag 92019, Auckland, New Zealand

9 ⁴ Lamont-Doherty Earth Observatory, Palisades, New York 10964, USA

10 ⁵ Department of Geological, Environmental, and Marine Sciences, Rider University, 2083 Lawrenceville Rd, Lawrenceville,
11 NJ, 08648, USA

12 ⁶ Department of Geography, University of Cambridge, Cambridge, UK

13 ⁷ School of Biological, Earth and Environmental Sciences, University of New South Wales, Sydney, NSW 2052, Australia

14 *Correspondence to:* Rob Wilson (rjsw@st-andrews.ac.uk)

15 **Abstract.** We evaluate a range of blue intensity (BI) tree-ring parameters in eight conifer species (12 sites) from Tasmania
16 and New Zealand for their dendroclimatic potential, and as surrogate wood anatomical proxies. Using a dataset of ca. 10-15
17 trees per site, we measured earlywood maximum blue intensity (EWB), latewood minimum blue intensity (LWB) and the
18 associated delta blue intensity (DB) parameter for dendrochronological analysis. No resin extraction was performed,
19 impacting low-frequency trends. Therefore, we focused only on the high-frequency signal by detrending all tree-ring and
20 climate data using a 20-year cubic smoothing spline. All BI parameters express low relative variance and weak signal
21 strength compared to ring-width. Correlation analysis and principal component regression experiments identified a weak and
22 variable climate response for most ring-width chronologies. However, for most sites, the EWB data, despite weak signal
23 strength, expressed strong coherence with summer temperatures. Significant correlations for LWB were also noted, but the
24 sign of the relationship for most species is opposite to that reported for all conifer species in the Northern Hemisphere. DB
25 results were mixed but performed better for the Tasmanian sites when combined through principal component regression
26 methods than for New Zealand. Using the full multi-species/parameter network, excellent summer temperature calibration
27 was identified for both Tasmania and New Zealand ranging from 52% to 78% explained variance for split periods (1901-
28 1950 / 1951-1995), with equally robust independent validation (Coefficient of Efficiency = 0.41 to 0.77). Comparison of the
29 Tasmanian BI reconstruction with a quantitative wood anatomical (QWA) reconstruction shows that these parameters record
30 essentially the same strong high-frequency summer temperature signal. Despite these excellent results, a substantial
31 challenge exists with the capture of potential secular scale climate trends. Although DB, band-pass and other signal
32 processing methods may help with this issue, substantially more experimentation is needed in conjunction with comparative
33 analysis with ring density and QWA measurements.

34 **1 Introduction**

35 The range of variables that are now routinely measured from the rings of trees, including width, stable isotopes, multiple
36 wood anatomical properties and density, has increased substantially in recent years (McCarroll et al. 2002; McCarroll and
37 Loader, 2004; Drew et al. 2013; von Arx et al. 2016; Björklund et al., 2020). However, our knowledge of the climatic,
38 environmental, and physiological processes that modulate the year-to-year variability of these different tree-ring parameters
39 is still far from comprehensive.

40

41 Since the early seminal work of Fritts et al. (1965), a well-known rule of thumb for ring-width (RW) based
42 dendroclimatology is that trees sampled near their high elevation or latitude treelines will be predominantly temperature
43 limited, while at lower elevations or latitudes, moisture limitation becomes the primary driver of growth (Fritts 1976;
44 Kienast et al. 1987; Buckley et al. 1997; Wilson and Hopfmüller 2001; Briffa et al., 2002; Babst et al. 2013; St. George
45 2014). Such targeted sampling is strategically vital in “traditional” dendroclimatology and robust reconstructions can be
46 derived so long as tree-line sites are sampled where a single dominant climate parameter controls growth (Bradley 1999).
47 However, the climatic influence on RW can be complex and there are many published studies where the relationship
48 between RW and climate is shown to be temporally unstable and/or non-linear (Wilmking et al. 2020).

49

50 Ring density parameters, especially maximum latewood density (MXD), have been shown to provide substantially more
51 robust estimates of past summer temperature compared to RW (Briffa et al., 2002; Wilson and Luckman, 2003; Esper et al.,
52 2012; Büntgen et al., 2017; Ljungqvist et al., 2020). Density data may also retain a strong temperature signal at elevations
53 below the upper treeline, minimising the non-linear influence of a changing tree-line elevation through time (Kienast et al.
54 1987). The use of ring-density variables from lower elevation or latitude sites to reconstruct past hydroclimate is rare
55 (Camarero et al. 2014, 2017; Cleaveland 1986; Seftigen et al. 2020) and is clearly an area demanding further attention.

56

57 The reconstructive value of tree ring stable isotopes (carbon and oxygen) appears to be less constrained for sites where
58 climate does not limit growth and substantial potential exists from mid-latitude regions where traditional
59 dendroclimatological approaches are less reliable (McCarroll and Loader, 2004; Loader et al. 2008; Young et al. 2015;
60 Loader et al. 2020; Büntgen et al. 2021). However, within the mechanistic framework of stable isotopes, there is still much
61 to explore regarding the complex associations between fractionation and climate for different species and across different
62 ecotones.

63

64 The use of quantitative wood anatomical (QWA) parameters for dendroclimatology has gained traction in recent years due to
65 improvements in measurement methodologies allowing for the development of well-replicated chronologies for multiple
66 different anatomical variables (Drew et al. 2013; von Arx et al. 2016; Prendin et al., 2017; Björklund et al. 2020). The

67 strength of relationships between climate parameters and wood anatomical properties such as latewood cell wall thickness,
68 tracheid radial diameter and microfibril angle is comparable to and can be stronger than maximum latewood density (Yasue
69 et al., 2000; Wang et al., 2002; Panyushkina et al., 2003; Fonti et al., 2013; Allen et al. 2018).

70
71 Despite the strong climate signal often noted in such non-RW tree-ring parameters, their procurement is expensive, often
72 requires specialised equipment and experience, and is time consuming. Consequently, there are substantially less published
73 data available for inspection and assessment. In recent years, blue intensity (BI) has been championed by many groups as a
74 cheaper surrogate for maximum latewood density (Björklund et al., 2014, 2015; Rydval et al., 2014; Wilson et al., 2014;
75 Kaczka and Wilson 2021). In its common usage, BI measures the intensity of the reflectance of blue light from the latewood
76 of scanned conifer samples so that a dense (dark) latewood would result in low-intensity values. MXD and BI essentially
77 measure similar wood properties. Most studies that have directly compared MXD and latewood BI show no significant
78 difference in the climate response of the two parameters (Wilson et al., 2014; Björklund et al. 2019; Ljungqvist et al., 2020;
79 Reid and Wilson 2020). Though the acceptance of BI in dendrochronology was initially slow after the publication of the
80 original concept paper (McCarroll et al. 2002), over the past decade many BI-based studies have been published (Kaczka and
81 Wilson 2021). These studies have examined the use of BI as an ecological and climatological indicator in a variety of conifer
82 species from several locations around the Northern Hemisphere (Campbell et al., 2007, 2011; Helama et al., 2013; Rydval et
83 al., 2014, 2017, 2018; Björklund et al., 2014, 2015; Wilson et al., 2014, 2017a, 2017b, 2019; Babst et al., 2016; Dolgova,
84 2016; Arbellay et al., 2018; Buras et al., 2018; Fuentes et al., 2018; Kaczka et al., 2018; Wiles et al., 2019; Harley et al.
85 2020; Heeter et al. 2020; Reid and Wilson 2020; Davi et al. 2021).

86
87 Only three studies that utilise BI data south of 30°N have been published. Buckley et al. (2018) explored the potential of
88 reflectance parameters from the tropical conifer Fujian cypress (*Fokienia hodginsii*) from central Vietnam and found a
89 significant positive relationship between earlywood maximum BI and December-April maximum temperature. Although a
90 spring/early summer temperature signal is extant in Northern Hemisphere conifer minimum density data from temperature
91 limited sites (Björklund et al. 2017), correlations are generally not as strong as the earlywood results detailed by Buckley et
92 al. (2018). In the Southern Hemisphere, Brookhouse and Graham (2016) measured latewood BI from *Errinundra plum-pine*
93 (*Podocarpus lawrencei*) samples taken from the Australian Alps and identified a strong inverse ($r = -0.79$) relationship with
94 August-April maximum temperatures, suggesting substantial potential for this species if long-lived specimens could be
95 found. Finally, Blake et al. (2020) recently explored the climate signal in BI parameters measured from Silver pine (*Manoao*
96 *colensoi*) samples growing on New Zealand's South Island and found strong significant relationships between both
97 earlywood and latewood BI parameters and summer temperatures. Although the sign (positive) of the earlywood BI
98 relationship with temperature agreed with results detailed in other studies (Björklund et al. 2017; Buckley et al. 2018), the
99 latewood relationship was inverse to that detailed for Northern Hemisphere conifers (Briffa et al. 2002) and observed by
100 Brookhouse and Graham (2016). This difference in latewood response begs the intriguing question as to whether some

101 Southern Hemisphere conifers may have evolved differently from their Northern Hemisphere counterparts, resulting in a
 102 different anatomical and physiological response to climate.

103

104 Here we expand upon the pilot studies of Brookhouse and Graham (2016) and Blake et al. (2020) and explore the climate
 105 signal of BI parameters from several key conifer species from Tasmania and New Zealand. To minimise nomenclature
 106 confusion, we refer to the different BI parameters as earlywood blue intensity (EWB) and latewood blue intensity (LWB).
 107 Based on ecophysiological theory (Buckley et al. 2018) we posit that EWB, derived from maximum intensity values of the
 108 whole-ring reflectance spectrum, essentially provides a surrogate for mean lumen size of the earlywood cells, while LWB,
 109 derived from minimum reflectance values, reflects the relative density (i.e. the proportion of cell wall to lumen area) of the
 110 darker latewood cell walls. We further suggest these reflectance measures are useful surrogate measures of mean tracheid
 111 diameter and cell wall thickness, which are proven to be excellent proxies of past climate (Allen et al. 2018; Björklund et al.
 112 2019) but are laborious and expensive to measure directly. As well as undertaking a dendroclimatic assessment of multiple
 113 BI parameters from different Australasian conifers, our analysis will also identify which species would be a good focus for
 114 further BI and QWA measurement in the future. Improving terrestrial-based estimates of past temperature in the land-limited
 115 Southern Hemisphere (Neukom et al. 2014) will only be achieved by enhancing the strength of the calibrated signal that until
 116 recently has been characterized solely by ring-width data which generally express a weak temperature signal.

117

Site Name	Site code	Common name	Species	Latitude (S)	Longitude	Elevation (m)	No of series	No of trees	full period	period ≥ 3 series
TASMANIA										
Race Spur	RCS	Celery Top pine	<i>Phyllocladus aspleniifolius</i>	41.29	145.44	500-550	16	14	1788-1995	1795-1995
L. Mackenzie	MCK	Pencil pine	<i>Athrotaxis cupressoides</i>	41.41	146.23	1116	15	15	1771-2007	1780-2007
Cradle Mountain	CM	Pencil pine	<i>Athrotaxis cupressoides</i>	41.40	145.57	1050	15	15	1787-2001	1789-2001
Mt Weld West / Trout Lake	MWWTRL	King Billy pine	<i>Athrotaxis selaginoides</i>	43.00	146.34	950	17	9	1781-1998	1785-1998
Mt Read - KBP	MRD	King Billy pine	<i>Athrotaxis selaginoides</i>	41.50	145.32	900	13	6	1770-2010	1778-2010
Mt Read - HP	MHP	Huon pine	<i>Lagarostrobos franklinii</i>	41.50	145.32	1000	22	16	781-2002	1238-2001
John Butters Power Station (King River)	BUT	Huon pine	<i>Lagarostrobos franklinii</i>	42.15	145.30	60	10	10	1773-2008	1798-2008
NEW ZEALAND										
Puketi	PKL	NZ Kauri	<i>Agathis australis</i>	35.15	173.45	180	13	10	1674-2001	1737-2001
Huapai	HUP	NZ Kauri	<i>Agathis australis</i>	36.48	174.3	100	17	13	1664-2007	1723-2006
Flagstaff	FLC	NZ Cedar	<i>Libocedrus bidwillii</i>	42.30	171.43	280	12	7	1774-2004	1776-2004
Ahaura	AHA	Silver pine	<i>Manoao colensoi</i>	42.23	171.48	244	12	12	1750-2012	1750-2012
Doughboy, Stewart Island	DPP	Pink pine	<i>Halocarpus biformis</i>	46.59	167.43	230	20	12	1767-2010	1777-2010

118

119

120 **Table 1: Chronology information for the seven Tasmanian and five New Zealand sites used in the study (see Figure 1).**

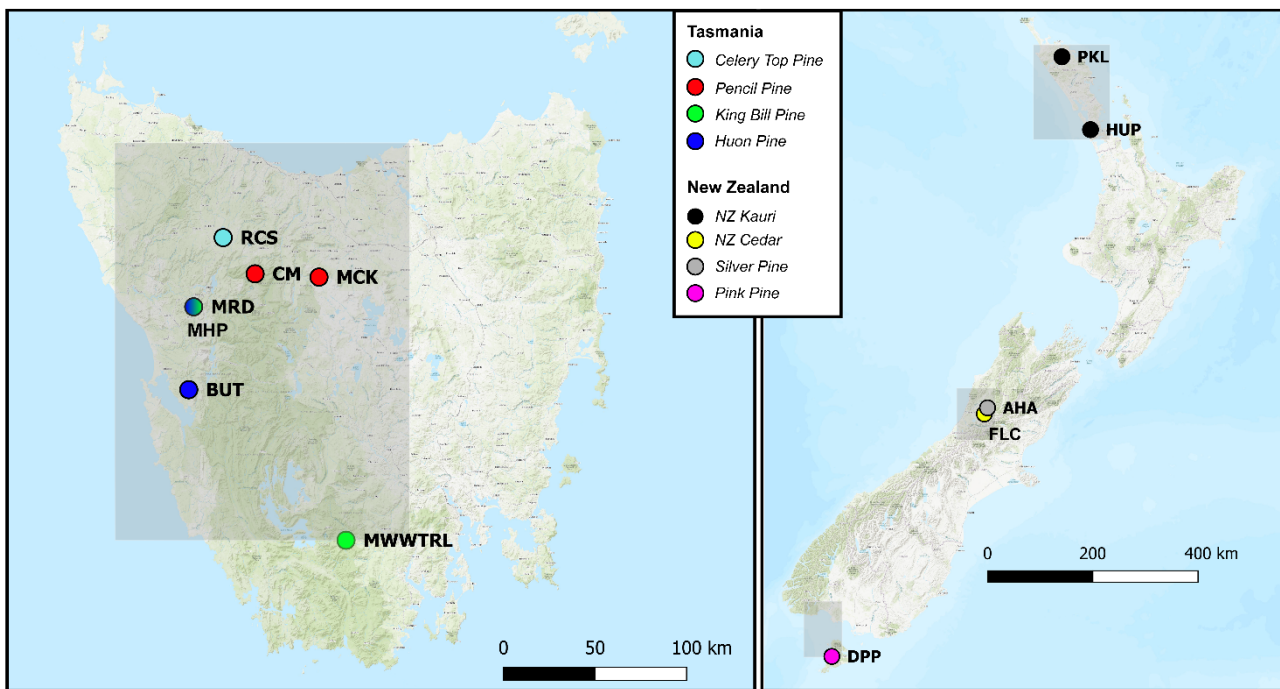
121

122 2 Data and Methods

123 Four tree species from Tasmania and four from New Zealand were targeted for analysis (Figure 1, Table 1) representing
 124 conifer species that have not only been the focus of previous dendrochronological studies, but each has the potential to
 125 produce climate proxy records substantially greater than 1000 years in length. Until recently, RW data were used for most

126 Australasian dendroclimatological studies, with calibration results never exceeding 40-45% explained variance. In Tasmania,
127 the strongest calibration results for summer temperatures had been obtained using high elevation Huon pine (*Lagarostrobos*
128 *franklinii* - Buckley et al. 1997; Cook et al. 2006) although some coherence was also found for Pencil pine (*Athrotaxis*
129 *cupressoides*) and King Billy pine (*Athrotaxis selaginoides* - Allen et al. 2011; Allen et al. 2017). The study sites (Table 1)
130 for Pencil pine (MCK and CM) and King Billy pine (MWWTRL and MRD) are located close to the upper timberline limit of
131 these species and growth is expected to be controlled mostly by summer temperatures. Likewise, the high elevation Huon
132 pine (MHP) site is also close to the upper treeline where summer temperature is the dominant response (Buckley et al. 1997).
133 However, BUT is located at the lower end of the Huon pine elevational range within a riparian environment so temperature
134 limitation is unlikely in a traditional sense. However, Drew et al (2013) identified strong summer temperature signals in
135 latewood QWA data for this site. Celery Top (*Phyllocladus aspleniifolius*) RW data, however, express a complex non-linear
136 relationship with climate along its species' elevational range and have not been used for dendroclimatic reconstruction
137 (Allen et al. 2001). By contrast, summer temperature calibration experiments performed on measurement series of several
138 wood anatomical properties (e.g. tracheid radial diameter, cell wall thickness and microfibril angle), as well as RW and ring
139 density, from these same species, have shown substantial improvement over RW alone (Allen et al. 2018), although these
140 QWA data have been more useful for hydroclimate reconstructions (Allen et al. 2015a/b). In New Zealand, RW-based
141 summer temperature reconstructions have been developed from NZ Cedar (*Libocedrus bidwillii* - Palmer and Xiong 2004),
142 Silver pine (*Manoao colensoi* - Cook et al. 2002, 2006) and Pink pine (*Halocarpus biformis* - D'Arrigo et al. 1996, Duncan
143 et al. 2010) although ring density (Xiong et al. 1998 – Pink pine) and BI (Blake et al. 2020 – Silver pine) measured from the
144 earlywood have produced stronger results. For this study, we specifically measured BI from samples used in previous,
145 mostly RW-based dendroclimatic, studies where summer temperature was found to be the dominant climate signal - at least
146 for NZ Cedar, Silver pine and Pink pine. The sites for these three New Zealand species are close to their southern
147 (latitudinal) limits (especially the Stewart Island Pink pine site) which is thought to compensate, to some degree, for their
148 modest elevational range (Table 1). Kauri (*Agathis australis*) is the longest-lived tree species in Australasia (Boswijk et al.
149 2014) but only a few sites of reasonably mature trees exist. Previous analyses have identified a complex mixed response to
150 both temperature and precipitation through the growing season (Buckley et al 2000, Fowler et al, 2000). However, it is
151 notable that Kauri RW data express a strong stable relationship with indices of the El Nino Southern Oscillation (Cook et al.
152 2006; Fowler et al. 2012).

153



154

155

156 **Figure 1: Location map (basemap ESRI 2021) of the tree-ring sites used in this study (see Table 1). Also indicated (grey boxes) are**
 157 **the regional domains of the gridded CRU TS 4.03 temperature and precipitation data (Harris et al., 2014) used for analyses.**
 158 **Tasmania: 145-147°E / 41-43°S; New Zealand: North: 173-175°E / 35-37°S; Central: 171-172°E / 42-43°S ; South: 167-168°E / 46-**
 159 **47°S.**

160

161

162 In this study, we utilised tree cores sampled over the past three decades that has been prepared for RW measurement.
 163 Considering the focus of this study is to assess the potential of BI parameters for enhancing dendroclimatic reconstruction,
 164 and the fact that the samples were already mounted, no resin extraction was performed except for the Silver pine AHA site
 165 (see Blake et al. 2020 for details). As many of the species are resinous by nature, this immediately imposes a potential
 166 problem for measuring BI data, because any inhomogeneous resin-related discolouration will impact intensity values
 167 (Rydval et al., 2014; Björklund et al., 2014, 2015; Wilson et al. 2017b; Reid and Wilson 2020). Consequently, as the high-
 168 frequency signal will only be minimally affected by discolouration (Wilson et al. 2017a), all analyses for this proof-of-
 169 concept study will utilise only the high-pass fraction of the chronologies.

170

171 The mounted samples were re-sanded using fine grade (> 600 grit) sandpaper to remove decadal markings. Samples were
 172 scanned at multiple institutions using different scanners and a range of resolutions from 1200 to 3200 DPI. RW and BI data
 173 were generated using Coorecorder (Cybis 2016, <http://www.cybis.se/forfun/dendro/index.htm>) except for AHA

174 (WinDendro – see Blake et al. 2020). Regardless of image resolution, the CooRecorder BI generation “window” was set to
175 roughly equate to two-thirds width of the sample while the window depth encompassed either the latewood or earlywood for
176 each ring. The BI data were extracted following the method detailed in Buckley et al. (2018). For LWB, mean reflectance
177 values were taken from the lowest 15% of the darkest pixels, while for EWB the mean of the brightest 85% of the pixels was
178 used. Despite many of the samples being substantially older, most samples were measured only back into the 17th or 18th
179 centuries (with site MHP (Table 1) being an exception), providing enough data to ensure robust calibration and validation
180 over the instrumental period and to allow comparison with a temperature reconstruction from Tasmania based on QWA data
181 (Allen et al. 2018). Parameters generated for analysis were RW, EWB and LWB. As the study focuses only on the high-
182 frequency signal extant in the tree-ring data, the LWB data were not inverted as is the norm in Northern Hemisphere studies
183 using data generated in CooRecorder (Rydval et al. 2014).

184

185 Perhaps the greatest limitation for BI data parameters is that any colour changes that do not represent year-to-year changes in
186 wood anatomical features such as lumen size and cell wall thickness will impose a colour-related bias in the intensity
187 measurements. Examples of non-anatomically related colour changes are those associated with the heartwood/sapwood
188 transition, sections of highly resinous wood, or fungal staining. Björklund et al. (2014) proposed a statistical procedure that
189 could correct for such colour changes. This procedure subtracts the LWB reflectance value from the EWB data producing a
190 delta parameter (hereafter referred to as Delta BI - DB). Theoretically, DB should correct for common colour change biases
191 between heartwood and sapwood and even resinous zones within the wood. To date, DB has been utilised successfully in
192 only a few studies (Björklund et al., 2014, 2015; Wilson et al., 2017b; Fuentes et al. 2018; Blake et al. 2020; Reid and
193 Wilson 2020). As no resin extraction was performed (except site AHA, Table 1) and all the species used for this study
194 express a colour change from heartwood to sapwood, DB data will also be examined to explore its high-frequency
195 dendroclimatic potential.

196

197 For some of the studied species, the heartwood/sapwood transition colour change is very sharp and pronounced in
198 reflectance values (Figure A1), and inflexible detrending options could impose a systematic bias in the resultant detrended
199 indices. As an extreme example, the heartwood/sapwood transition of the EWB raw mean non-detrended chronology for the
200 CM Pencil pine site (Figure A2) cannot be tracked well with cubic smoothing splines (Cook and Peters 1981) of 200, 100 or
201 even 50 years respectively. This is not surprising given that the smoothing spline, operating as a symmetric digital filter, is
202 not well suited for dealing with abrupt changes in time series such as that observed in the CMewb chronology. In fact, the
203 bias of low (pre-transition) and high (post- transition) index values are only minimised when a flexible 20-year spline is used
204 because it better adapts to the observed discontinuity. However, this adaptability comes at the cost of losing potentially
205 valuable >20-year variability in the time series. This is clearly undesirable and better ways of modelling and removing such
206 discontinuities without the unwanted loss of lower-frequency variability are needed (see later discussion). Although less

207 flexible splines could be used for other species with a gradual or minimal colour change from heartwood to sapwood (Figure
208 A1), a consistent approach to detrending was deemed prudent and therefore a 20-year spline was used for all datasets.
209

210 The mean interseries correlation statistic (R_{BAR}) is utilised to assess how many series are needed to attain an Expressed
211 Population Signal value of 0.85 (Wigley et al. 1984; Wilson and Elling 2004). Previous research has shown that the common
212 signal expressed by BI data can be rather weak (Wilson et al. 2014, 2017a/b, 2019; Kaczka et al. 2018; Wiles et al. 2019).
213 We explore this phenomenon further with this multi-parameter/species network by using the coefficient of variation to help
214 understand relative internal variance and covariance of the parameter chronologies.
215

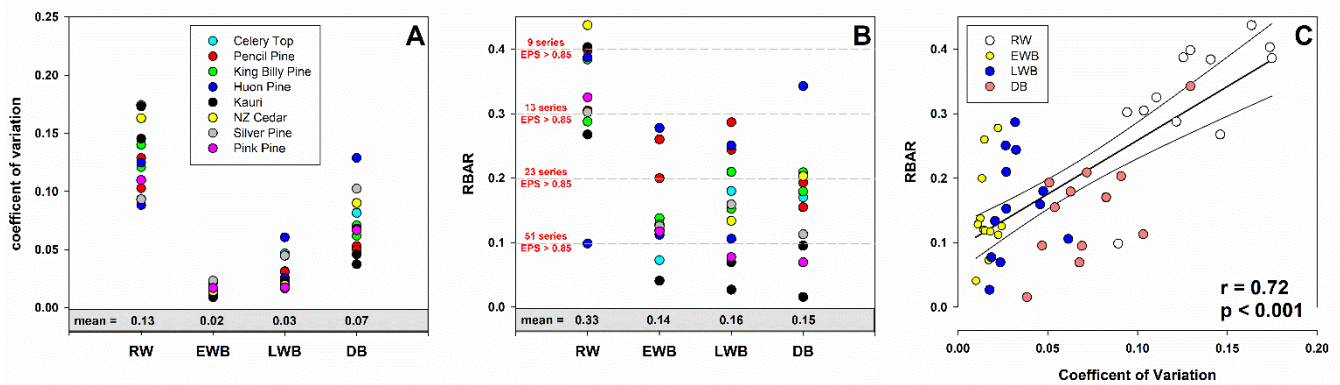
216 The climate signal expressed in the individual chronologies was initially explored using simple correlation analysis against
217 monthly gridded (see Figure 1 for locations) CRUTS 4.03 temperature and precipitation data (Harris et al. 2014) for the
218 periods 1902-1995, 1902-1950 and 1951-1995. Although the CRU TS data start in 1901, 1902 was the initial start year as
219 correlations were performed over 20 months including the previous growing season while 1995 reflects the final common
220 year for all tree-ring datasets (Table 1). The climate data were similarly detrended as the tree-ring data to ensure consistency.
221 Unsurprisingly, as most of the study sites are located in temperature limited upper tree-line locations, correlations with
222 monthly precipitation were weak, variable and temporally unstable for all species/parameter chronologies studies. The
223 results are presented in the Appendix but are not discussed further (see Table A4a-d).
224

225 Principal component analysis (PCA) was used on varying subsets of chronologies for each region (i.e. all chronologies of the
226 same parameter, or all parameters from a single species) to reduce the data to a few modes of common variance. Principal
227 components that had both an eigenvalue > 1.0 and correlated significantly (95% C.L.) with the target instrumental data were
228 entered into a stepwise multiple regression and calibrated against a range of seasonal temperatures. For New Zealand, the
229 three CRU TS 4.03 grid boxes (Figure 1) were averaged to create a countrywide mean series. This was justified as the three
230 inter-grid boxes mean correlation values between all tested seasons was 0.93 (STDEV = 0.01) suggesting there is a strong
231 common temperature signal between North Island and southern South Island. PCA was also utilised to ascertain the optimal
232 season for dendroclimatic calibration using the full chronology network for each country as well as exploring seasonal
233 differences between parameters and species. Analyses were performed over the common period of all tree-ring and climate
234 data (1901-1995) as well as early (1901-1950) and late (1951-1995) period calibration and verification. The Coefficient of
235 Efficiency (CE - Cook et al., 1994) was used to validate the regression-based climate estimates.

237 3.1 Chronology variability and signal strength

238 Wilson et al. (2014), using upper tree-line temperature-sensitive spruce samples from British Columbia, noted lower mean
 239 coefficient of variation (CV) values for LWB (0.05) compared to RW (0.28) and MXD (0.19). Common signal strength was
 240 strongest for the MXD data (RBAR = 0.42) while RW and LWB expressed similar but lower values (0.30). For the
 241 Australasian detrended data, overall, RW data express higher relative variance (mean CV = 0.13) followed by DB (0.07),
 242 LWB (0.03) and EWB (0.02 – Figure 2a). The range in values for RW (0.09 – 0.17) and DB (0.04 - 0.13) are greater than
 243 LWB (0.02 - 0.06) although there is overlap in the range of DB and LWB. The EWB data express a significantly narrower
 244 range (0.01 - 0.02). RBAR values for the four different parameter groups generally return a stronger common signal for RW
 245 (mean = 0.33) compared with EWB (0.14), LWB (0.16), and DB (0.15 – Figure 2b). Therefore, following traditional
 246 methodologies to assess signal strength, more BI series are needed than RW to attain a robust chronology. On average across
 247 all sites, to attain an EPS value of at least 0.85 (Wigley et al. 1984), 14 series would be needed for RW, while 44, 47 and 58
 248 series would be needed for EWB, LWB and DB respectively. This weaker common signal of the BI parameters has been
 249 noted before (Wilson et al. 2014, 2017a/b, 2019; Kaczka et al. 2018; Wiles et al. 2019; Blake et al. 2020) and is also noted in
 250 QWA data from Tasmania (Allen et al. *in prep*). The common signal is particularly weak for Celery Top and Kauri (EWB)
 251 and Pink pine and Kauri (LWB and DB – see Table A1 for detailed values).

252



253

254 **Figure 2: A. Coefficient of variation (CV) of the 20-year spline detrended chronologies; B: mean inter-series correlation (RBAR) of**
 255 **the 20-year spline detrended series. Horizontal dashed lines denote the number of series needed for that particular RBAR value to**
 256 **attain an EPS of 0.85; C: Scatter plot of CV versus RBAR with linear regression.**

257

258 A scatter plot of the CV and RBAR data (Figure 2c) suggests that the common signal expressed by these chronologies is
 259 partly a function of the relative variance of the time-series ($r = 0.72$, $p < 0.001$). Although the range in RBAR values for the
 260 EWB and LWB data suggests some uncertainty in this observation (see also Table A1), these results imply that the relatively

261 low variation of values around the mean for the BI parameters suggests that any anomalous colour staining on the wood that
262 does not reflect the true wood properties being measured could have a substantial impact on the chronology common signal.
263 However, it should be emphasised that a weak common signal and low EPS value does not necessarily result in a weak
264 climate signal (Buras 2017).

265 **3.2 Climate response**

266 The strength of correlations between the RW chronologies and mean monthly temperatures vary in sign and strength across
267 species. Over the full 1902-1995 period (Table 2), the Tasmanian MWWTRL (King Billy pine) and MHP (high elevation
268 Huon pine) sites express significant positive correlations with September-February and January-February respectively,
269 which are broadly time stable (Table A3a). RCS (Celery Top pine), MCK (Pencil pine) and MRD (King Billy pine) show
270 inverse correlations with late summer temperatures of the previous year. Of the New Zealand sites, PKL (Kauri) has negative
271 correlations for many months from winter through to the summer, while AHA (Silver pine) and DPP (Pink pine) correlate
272 positively with December-April and September- November.

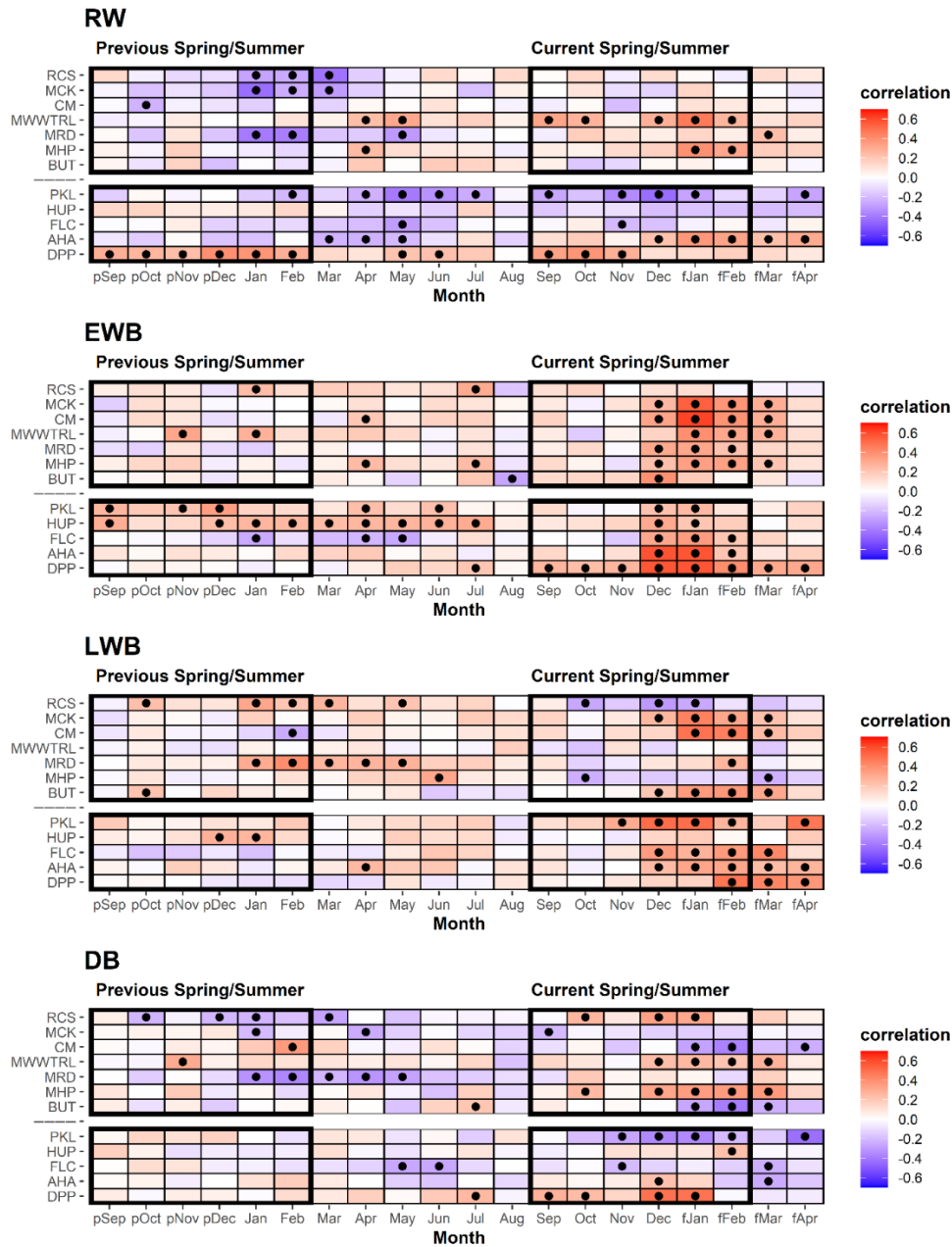
273

274 Correlations between the EWB chronologies and mean temperatures are surprisingly consistent for most sites although
275 correlations for RCS (Celery Top pine) and BUT (low elevation Huon pine) are weak. Almost all site chronologies correlate
276 positively with the summer months for the current season – December through to March (Tasmania) and December-February
277 (New Zealand). The King Billy pine and Kauri sites express narrower (MMWTRL, MRD, PKL, and HUP) response
278 windows while DPP (Pink pine) is wider (Table 2). Although these relationships appear generally time stable, the Tasmanian
279 sites correlate more strongly with the narrower January-February season for 1902-1950 compared to the later post-1951
280 period (Table A3b). Significant correlations with winter and prior year temperatures are weaker and less consistent than for
281 current spring/summer. Overall, the consistent and strong correlations of EWB with summer temperatures are extremely
282 encouraging and show great promise for enhancing RW-based temperature reconstruction for both regions.

283

284 Significant relationships between LWB and summer and early Autumn temperatures are generally noted, although the results
285 are less consistent than those for EWB. Both RCS (Celery Top) and high elevation Huon pine (MHP) express negative
286 correlations that are in line with the positive MXD/temperature relationships noted in the Northern Hemisphere as the LWB
287 data are not inverted. Excluding MMWTRL (King Billy pine) and HUP (Kauri), which do not have any significant
288 correlations with temperature in the growing season, all the LWB chronologies express positive correlations with summer
289 and early autumn temperatures. This antithetic behaviour is not a new observation and has been noted by Drew et al. (2013),
290 O'Donnell et al. (2016), Blake et al. (2020) for latewood anatomical parameters and LWB data, but these new results suggest
291 that this physiological phenomenon is not based on a chance occurrence of a single species and is consistent between several
292 Australasian conifer tree species (Pencil pine, Huon pine (low elevation), Kauri, NZ Cedar, Silver pine and Pink pine). Blake

293 et al. (2020) explained the inverse LWB relationship as a reduction in the duration of secondary cell wall thickening in
 294 warmer years. Such “emergent” surprising results (Cook and Pederson 2011) clearly need further research and testing.
 295



296

297 **Table 2: Correlation response function analysis results for the different TR parameter chronologies with CRU TS temperatures.**
 298 **Analysis undertaken over the 1902-1995 period (see supplementary figure S3 for correlations for split periods 1902-1950, 1951-**
 299 **1995). The upper block is for the Tasmanian sites, while the lower block is New Zealand. See Table 1 for site code names and**
 300 **species. Black dots denoted correlations significant at the 95% C.L.**

301

302 The DB chronologies express a range of responses to temperature that are all generally weaker than for EWB and LWB
303 (Table 2). Significant positive correlations with summer temperatures are found for RCS (Celery Top), MMWTRL (King
304 Billy pine), MHP (Huon pine), and DPP (Pink pine). HUP (Kauri) and AHA (Silver pine) also express some weak positive
305 summer temperature coherence. Negative correlations are noted for CM (Pencil pine), BUT (low elevation Huon pine), PKL
306 (Kauri) and FLC (NZ Cedar). However, many of these correlations are not temporally stable when compared over the 1902-
307 1950 and 1951-1995 periods (Table A3d). Current theory suggests that DB should perform well when EWB and LWB
308 parameters are weakly correlated and express different earlier and later seasonal climate responses (Björklund et al., 2014).
309 However, the results herein indicate that this simple hypothesis does not consistently apply in this multi-species study. For
310 example, the EWB and LWB data for the Pink pine DPP site express different early (Sep-April) and late (Feb-Apr) seasonal
311 responses with temperatures (Table 2), but still show a reasonably high inter-parameter correlation (0.60, Table A2) although
312 this is partly expected as the response windows overlap. However, the DB data still expresses a significant and strong
313 response with summer temperatures, although marginally weaker than the EWB response. On the other hand, DB for the
314 Pencil pine sites (MCK and CM) behaves more like conifers in the Northern Hemisphere (Björklund et al., 2014; Wilson et
315 al. 2017b), with significant correlations noted for both EWB and LWB with summer temperatures, but, likely due to the high
316 inter-parameter correlation (0.57 and 0.68), the DB data express weak, or even inverse correlations with summer
317 temperatures. Overall, the DB results are mixed and disappointing. This parameter theoretically could minimise the colour
318 bias of the darker to lighter colour heartwood/sapwood transition (Figure A1) but, for the data used herein, as the high-
319 frequency signal often portrays a mixed or weak signal with temperature, it suggests that the DB parameter might not be a
320 valid approach to address the heartwood/sapwood transition bias. These results suggest that alternative approaches to using
321 DB may need to be explored to minimise the impact of the heartwood/sapwood change noted in most of the species used in
322 this study.

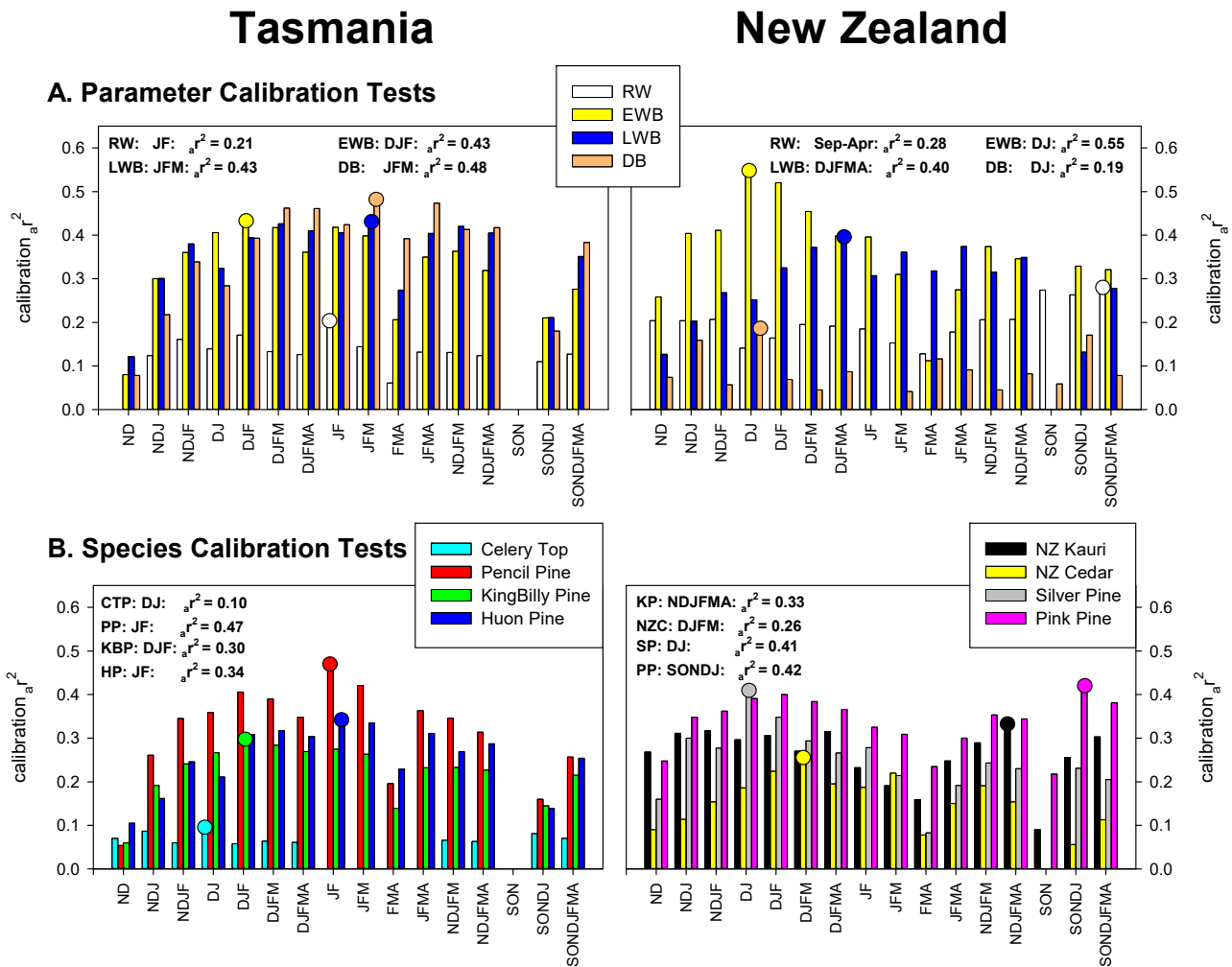
323 **3.3 Parameter and species-specific principal component calibration tests**

324 The previous section detailed that temperature is the predominant climate signal expressed across the Tasmanian and New
325 Zealand RW and BI data studied herein (Figures 3, A3a-d). Only weak coherence with precipitation was found (Table A4a-
326 d). To further explore the climate response, principal component regression calibration (1901-1995) experiments with
327 seasonal temperature were performed to ascertain which combination of BI parameters and species express the strongest
328 climate signal and therefore should be the focus for future research – including refined BI measurement and/or QWA
329 measurement.

330

331 For Tasmania, the PCA identifies three (RW), two (EWB), two (LWB) and two (DB) principal components respectively.
332 Each BI parameter PC regression explains > 40% of the temperature variance while RW is substantially weaker at 21%
333 (Figure 3a). Both EWB and LWB explain 43% of the December-February and January-March variance respectively - these

334 seasons being biologically logical with respect to the earlier seasonal start for EWB and later end for LWB. Despite the site-
 335 specific DB data correlating with temperature more weakly than EWB and LWB (Table 2), their multivariate combination
 336 calibrates better (48%) with January-March temperatures. Although this is an encouraging result as DB may theoretically
 337 correct for colour related biases, the mix of positive and negative zero-order correlations with temperature (Table 2) suggest
 338 that some caution will be needed if such data are used to capture more secular scale information.
 339



340
 341 **Figure 3: PC regression calibration (1901-1995) experiments for parameters (all species) (A) and species (all variables) (B). A**
 342 **range of temperature seasonal targets are used with the strongest seasonal calibrations highlighted with circles.**

343
 344 For New Zealand, PCA identifies 3, 2, 2 and 3 significant principal components for RW, EWB, LWB and DB respectively.
 345 EWB calibrates very strongly (55%) with December-January temperatures while LWB explains 40% of the broader

346 December-April season (Figure 3a). Alone, RW explains 28% of the temperature variance but for a broad September-April
347 season which reflects the variable site-specific responses of PKL, AHA and DPP (Table 2). The DB data calibrate poorly
348 explaining only 19% of the December-January temperature variance.

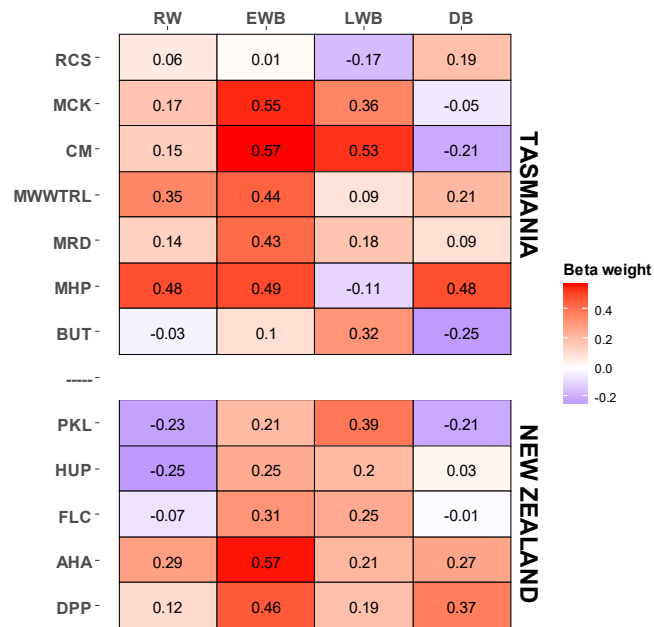
349

350 Of all the species tested, Tasmanian Pencil pine returns the strongest calibration (47%) with January-February temperatures
351 (Figure 3b) although New Zealand Silver pine and Pink pine also calibrate reasonably with 41% (December-January) and
352 42% (September-January). It should be noted that two Pencil pine sites were used (Table 1) compared to only one each for
353 Silver pine and Pink pine which likely will influence these results. King Billy pine, Huon pine and Kauri explain 30%
354 (December-February), 34% (January-February) and 33% (November-April) respectively of the temperature variance with
355 New Zealand cedar still showing some reasonable coherence (26%) for December-March. Celery Top is the weakest species
356 explaining only 10% of the December-January temperature variance.

357 **3.4 Region-wide calibration and validation**

358 A multi-site, multi-species approach to dendroclimatology can improve overall calibration even if some of the sampled sites
359 and species are not located close to climate limited treeline ecotones (Alexander et al. 2019). Herein we have an opportunity
360 to pool all the data for each country to create combined multi-species and multi-parameter regional reconstructions. As the
361 optimal season for calibration varies as a function of species and parameter (Figure 3), initial PC regression experiments,
362 using all chronologies from each of the two regions, were performed. For each of these models, all PCs with an eigenvalue
363 > 1.0 were entered into the regression model. January-February (JF) temperature was identified as the overall optimal season
364 for Tasmania while December-January (DJ) provided the strongest calibration for New Zealand. Forcing all variables into
365 the PC regression model also provides an opportunity to identify the importance of each species parameter towards the
366 development of regional reconstructions. The beta weights (Cook et al. 1994) from the regression modelling (Table 3)
367 clearly show the strong influence of the EWB parameters in the multiple regression model, especially from Pencil pine
368 (MCK and CM) and Silver pine (AHA) although strong beta weights are also noted for King Billy pine (MDR), Huon pine
369 (MHP) and Pink pine (DPP). Other parameters that provide useful information in the modelling are RW (King Billy pine
370 (MWWTRL) and Huon pine (MHP)), LWB (Pencil pine (MCK, CM), Huon pine (BUT) and Kauri (PKL)) and DB (Huon
371 pine (MHP) and Pink pine DPP)). These results are consistent with the correlation response function analysis (Table 2), but
372 it must be emphasised that the results shown in Table 3 are related to specific seasons (JF for Tasmania and DJ for New
373 Zealand) and may not reflect the optimal season for individual species or parameters (Figure 3).

374



375

376

377 **Table 3: PC regression calibration (1901-1995) beta weights using all parameter and species data. The Tasmanian modelling was**
 378 **performed against January-February temperatures while New Zealand was with December-January.**

379

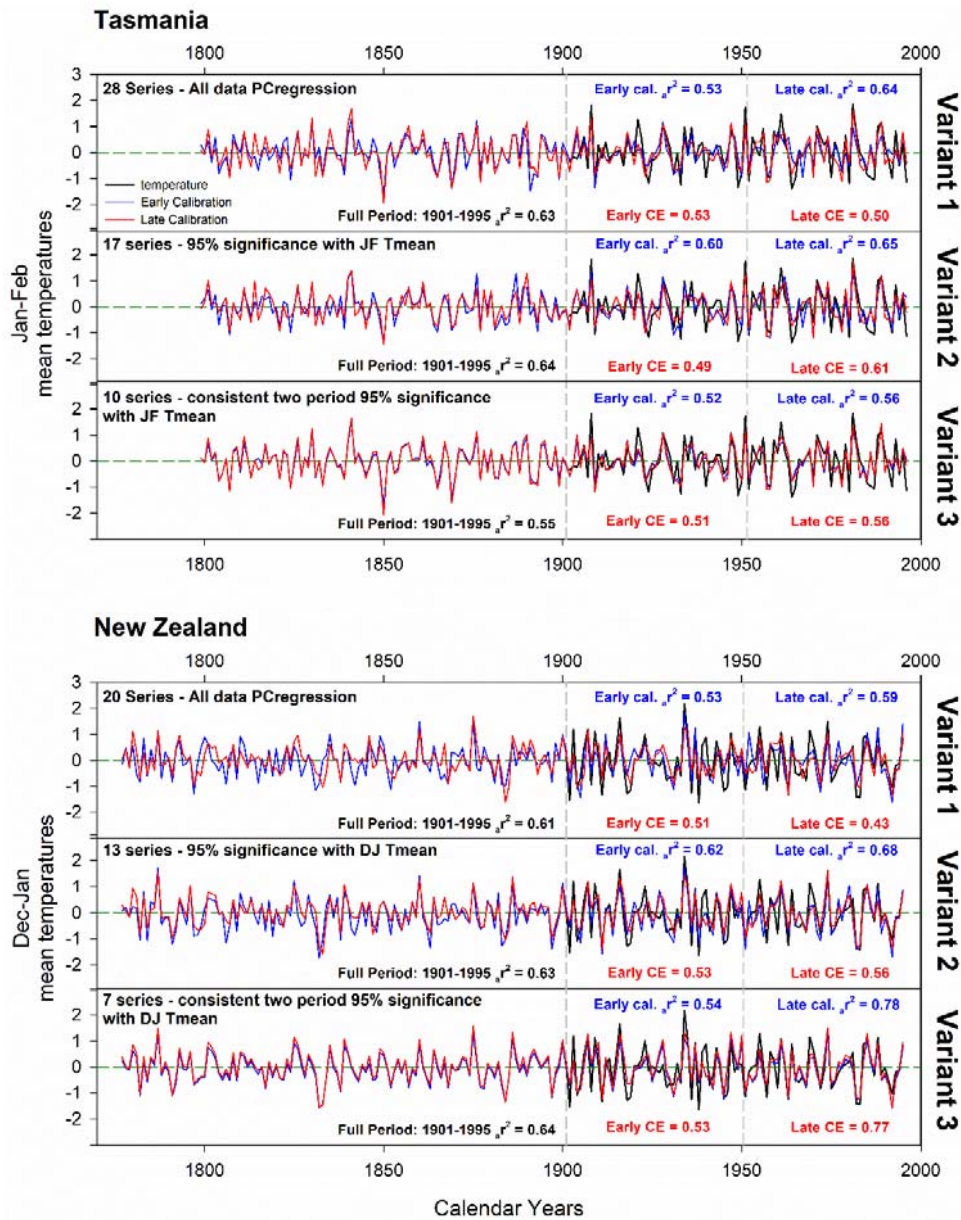
380

381 For the final countrywide calibration and validation experiments, three PC regression approaches were used, each reflecting
 382 more stringent screening procedures; (1) as already detailed above - all data entered into PCA and PCs with an eigenvalue >
 383 1.0 that correlated significantly (95%) with the instrumental target were entered as possible candidates into a stepwise
 384 multiple regression; (2) same as (1) but chronologies were initially screened for significant correlation with the full period
 385 instrumental target before PCA; (3) similar to previous variants, but significant consistent correlations between the
 386 chronologies and the instrumental target for both the 1901-1950 and 1951-1995 periods were required.

387

388 For Tasmania, the initial 28 parameter chronologies were reduced to 17 and 10 respectively via the two more stringent
 389 screening procedures while the 20 initial chronologies from New Zealand were reduced to 13 and 7 respectively (Figure 4).
 390 Full period (1901-1995) calibration is excellent for all versions with the Tasmanian variants 1 and 2 expressing 63-64% of
 391 the JF temperature variance, reducing to 55% for variant 3. The New Zealand data return similarly good results with 61-64%
 392 of the DJ temperature variance being explained by all variants. Split period calibration and validation are equally good for all
 393 variants with the Tasmanian variants explaining 52-65% of the variance for all early/late period calibration while CE ranges
 394 from 0.49-0.61. Similar results are obtained for New Zealand with calibration adjusted r^2 (a_r^2) and CE values ranging from

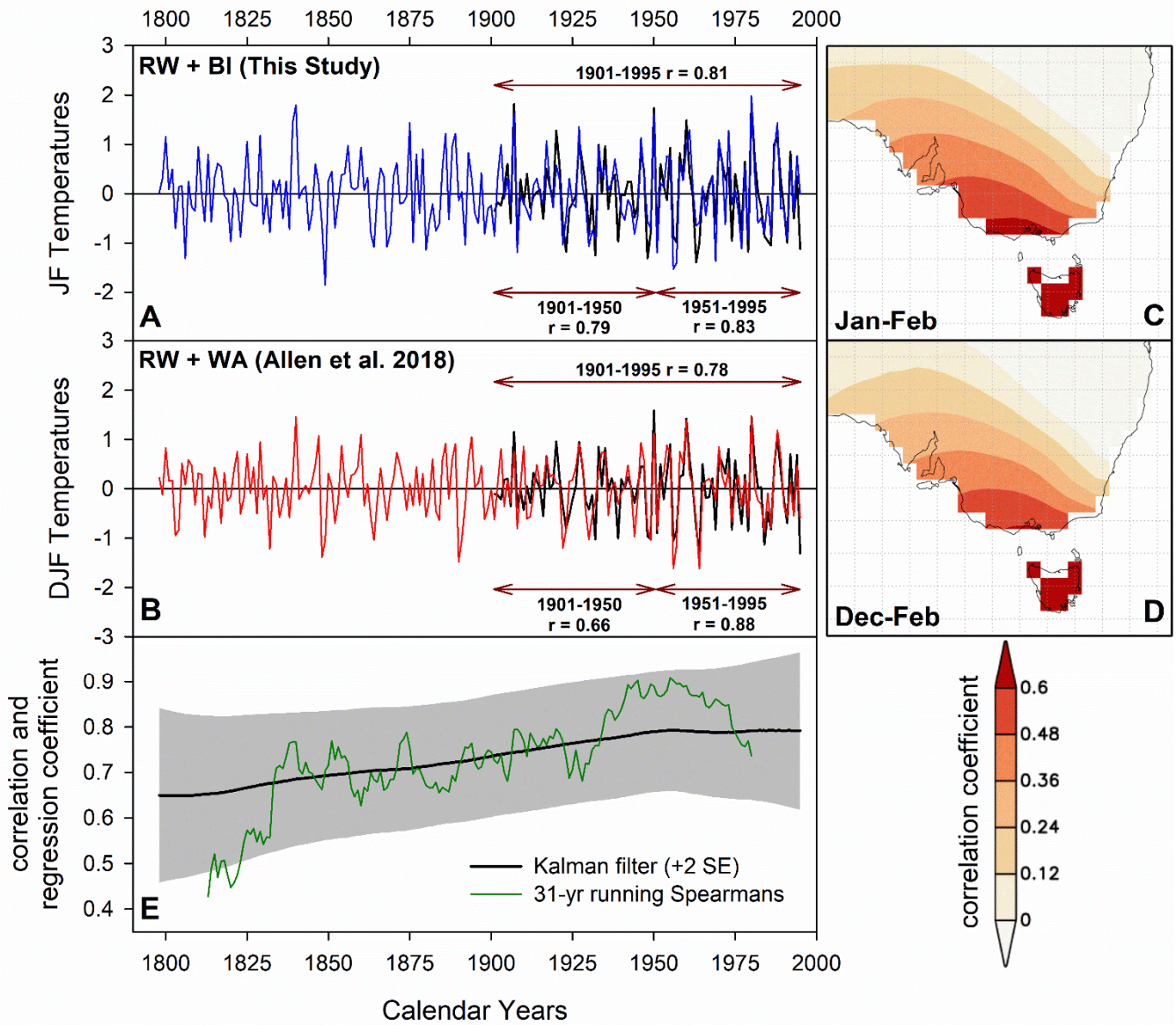
395 0.53-0.78 and 0.43-0.77 respectively. For both countries, calibration and validation are marginally stronger for the later
 396 1951-1995 period which might suggest some degree of uncertainty in the instrumental period in the early part of the 20th
 397 century.
 398



399

400

401 **Figure 4: Principal component regression results using all data (Variant 1), full period (1901-1995) screened data (Variant 2), and**
 402 **two-period screening (Variant 3). Split period calibration and validation were performed over 1901-1950 and 1951-1995.**



403

404

405 **Figure 5: A: Variant 2 (full period screened) Tasmanian JF temperature RW+BI parameter-based reconstruction with CRU TS**
 406 **temperature data. Pearson's correlation is shown for 1901-1995, 1901-1950 and 1951-1995 period; B: As A, but for Allen et al.**
 407 **(2018) RW+WA based Tasmanian DJF temperature reconstruction. These data have also been high-pass filtered using a 20-year**
 408 **cubic smoothing spline; C + D: Spatial correlations (1841-1995) between each reconstruction and similarly detrended Berkeley**
 409 **gridded data for the Jan-Feb and Dec-Feb seasons respectively; E: Running 31-year Spearman's rank correlation and Kalman**
 410 **filter analysis (Visser and Molenaar 1988).**

411

412 Overall, the temperature reconstruction experiments for both Tasmania and New Zealand (Figure 4) return excellent results
413 with overall calibration r^2 values well above 0.60. Although no QWA data exist yet for New Zealand, Allen et al. (2018)
414 recently produced a range of PC regression-based Tasmanian summer temperature reconstructions from a network of 58
415 chronologies using RW and QWA (mean tracheid radial diameter, mean cell wall thickness, mean density and microfibril
416 angle). These variables were measured using the SilviScan system (Evans, 1994) from the same four Tasmanian tree species
417 used herein using samples from the same region, but from more sites. Strong calibration results explaining 50-60% of the
418 temperature variance and robust validation were also noted in their analyses. We compare our full period screened
419 temperature reconstruction (Variant 2, Figure 4 – representing the most used data screening approach in dendroclimatology)
420 with a high-pass filtered (20-year spline) version of Allen et al.'s (2018) "Berkeley all-data" reconstruction variant (Figure
421 5). Both reconstructions correlate similarly with the CRU TS temperature data (1901-1995: RW/BI $r = 0.81$ (JF) and
422 RW/WA $r = 0.78$ (DJF) – Figure 5a/b) although the BI-based reconstruction expresses a slightly more stable response with
423 temperatures over the 1901-1950 and 1951-1995 periods ($r = 0.79$ and 0.83 vs 0.66 vs 0.88). However, as the BI-based
424 reconstruction was calibrated against these CRU TS data, this slight difference may simply reflect the optimised PC
425 regression fit to one instrumental dataset over another. Equivalent split period correlations using the Berkeley temperature
426 data (Rohde et al. 2013), as used by Allen et al. (2018), are $0.82/0.86$ (RW/BI) and $0.77-0.90$ (RW/WA).

427

428 Correlation with the Berkeley data over the 1841-1900 period, shows that coherence is weaker but similar between Allen et
429 al.'s (2018) and this study (0.54 and 0.66). The spatial representation of the reconstructed temperature signal in both datasets
430 is almost identical when using linearly detrended Berkeley gridded temperature data (Rohde et al. 2013) even when
431 including data back to 1841 (Figure 5c/d). Both reconstructions are strongly correlated with each other (Pearson's $r = 0.75$,
432 1798-1995) although this coherence weakens back in time as evidenced by both a running 31-year Spearman's rank
433 correlation and Kalman filter (Visser and Molenaar 1988), showing a peak coherence in the 20th century that decreases back
434 towards the early part of the 19th century (Figure 5e). This likely represents the decrease in sample replication through time
435 in some BI-based datasets (MWWTRL and BUT) used in this study (Figure A1). Overall, the BI data, at least for Tasmania,
436 basically express the same high-frequency signal as the WA data used in Allen et al. (2018) and the results herein suggest
437 that BI parameters could provide excellent proxies of past growing season temperatures. However, for their potential to be
438 truly realised, the heartwood/sapwood colour change and other discolouration issues need to be overcome.

439 **4 Conclusions and future research directions**

440 In this study, we measured a range of blue intensity parameters from eight conifer species from Tasmania and New Zealand
441 to ascertain whether the use of EWB, LWB and/or DB can improve upon previous RW-only based dendroclimatic
442 reconstructions that explain about 40-45% of the temperature variance. No attempt to remove resins was made for this proof-
443 of-concept study. Therefore, due to the impact on intensity-based parameters of resins and heartwood/sapwood colour

444 changes on the wood, we detrended the chronologies and climate data using a very flexible spline (20-years) to focus only on
445 the high-frequency signal. Metrics denoting signal strength (RBAR and EPS) indicated a very weak common signal in the BI
446 parameters (mean RBAR range 0.14 – 0.16, Figure 2b) compared to the RW data (mean RBAR = 0.33) which appeared to be
447 partly related to the relative variance in these datasets. The EWB data in particular exhibit very low variability which may
448 mean that any colour variation in the wood that does not reflect true year-to-year wood anatomical variance may have a large
449 impact on such data, thus weakening the common signal.

450

451 Despite the weak common signal expressed by the BI parameters, the climate signal extant in these data is very strong,
452 especially EWB. When all parameters are combined using PC regression, depending on the period used, 52-78% of the
453 summer temperature variance can be explained (Figure 4). This is generally greater than the norm for Northern Hemisphere
454 based MXD/BI-related temperature reconstructions (Wilson et al. 2016), although admittedly, the results in this study are
455 focused only on the high-frequency fraction of the data. These strong calibration results are driven mainly by EWB data
456 from Pencil pine, high elevation Huon pine and King Billy pine (Tasmania) and Silver pine, Pink pine and cedar (New
457 Zealand) although useful information was also identified in LWB (Pencil pine, low elevation Huon pine, Kauri and cedar),
458 DB (high elevation Huon pine and Pink pine) and RW (high elevation Huon pine – Table 3). However, the relationship of
459 LWB for most species with summer temperatures is opposite to that observed in the Northern Hemisphere and further study
460 is needed to assess the physiological processes leading to this inverse relationship in these particular Southern Hemisphere
461 conifers.

462

463 The similarity of the Tasmanian multi-TR-proxy reconstruction with a reconstruction heavily dependent on QWA data
464 (Allen et al. (2018) - Figure 5) clearly highlights that the BI and WA data express similar wood properties. This is a highly
465 encouraging result for the utilisation of BI as it is quicker and cheaper to produce than QWA data. However, the “elephant in
466 the room” is whether robust low-frequency information can be extracted from BI-based parameters or is it an analytical
467 methodology that ultimately will be relevant only for decadal and higher frequencies. It is unlikely that the
468 heartwood/sapwood colour change (both sharp and gradual – Figure A1), expressed by most of the tree species used in this
469 study, can be fully removed by resin extraction alone. Some success at overcoming heartwood/sapwood colour bias using
470 DB has been shown for some Northern Hemisphere conifer species (Björklund et al., 2014, 2015; Wilson et al., 2017b;
471 Fuentes et al. 2018; Reid and Wilson 2020), but the DB results detailed herein (Table 3, Figures 2- 4) suggest that DB may
472 not always provide a robust solution to the issue.

473

474 Other statistical approaches have been used to overcome the colour bias using either contrast adjustments (Björklund et al.,
475 2015; Fuentes et al., 2018) or band-pass approaches where the low-frequency signal is derived from the RW data and the
476 high frequency is driven by the BI data (Rydval et al., 2017) but further experimentation is needed. We hypothesise that
477 relatively sharp changes in colour intensity measures related to the heartwood/sapwood transition can be viewed

478 conceptually in a similar way to how endogenous disturbances affect ring-width parameters over time (Cook 1987). Similar
479 to the progress in developing growth release detection methods to reconstruct canopy disturbance histories of forests
480 (Altman 2020, Trotsiuk et al. 2018), radial growth averaging (Lorimer and Frelich 1989) or time series methods
481 (Druckenbrod et al., 2013; Rydval et al. 2016) could be used to identify and remove the colour bias signature resulting from
482 the change in physiology from heartwood to sapwood. However, to facilitate such signal processing methods, more studies
483 are needed to directly compare both MXD and QWA data with BI parameters to understand the secular trend biases in these
484 light intensity parameters. At the very least, the results detailed herein, based on a limited number of sites per species, show
485 that BI parameters can be used to identify those species that should be targeted for more costly and time-consuming
486 analytical methods such as QWA measurement.

SITE code	Mean value	CV	RBAR	n-EPS (0.85)
TASMANIA				
RCSrw	0.72	0.17	0.39	9.0
RCSewb	1.02	0.02	0.07	70.2
RCSlwb	0.58	0.05	0.18	25.6
RCSdb	0.45	0.08	0.17	27.3
MCKrw	0.75	0.13	0.40	8.5
MCKewb	1.19	0.01	0.20	22.5
MCKlwb	0.78	0.03	0.25	17.4
MCKdb	0.40	0.05	0.16	30.6
CMrw	0.71	0.10	0.31	12.9
CMewb	1.22	0.01	0.26	16.0
CMlwb	0.84	0.03	0.29	14.0
CMdb	0.36	0.05	0.19	23.5
MWWTRLrw	0.59	0.12	0.29	14.0
MWWTRLewb	1.23	0.01	0.14	34.9
MWWTRLlwb	0.82	0.03	0.15	31.1
MWWTRLdb	0.33	0.06	0.18	25.7
MRDrw	0.60	0.14	0.38	9.1
MRDewb	1.28	0.01	0.13	37.9
MRDlwb	0.88	0.03	0.21	21.2
MRDdb	0.40	0.07	0.21	21.3
MHPrw	0.36	0.13	0.39	8.9
MHPewb	1.06	0.02	0.28	14.7
MHPlwb	0.82	0.03	0.25	16.8
MHPdb	0.24	0.13	0.34	10.8
BUTrw	0.99	0.09	0.10	50.8
BUTewb	1.18	0.02	0.11	44.1
BUTlwb	0.63	0.06	0.11	47.0
BUTdb	0.58	0.07	0.10	52.9
NEW ZEALAND				
PKLrw	1.16	0.17	0.40	8.4
PKLewb	1.17	0.01	0.12	40.9
PKLlwb	0.83	0.02	0.07	73.7
PKLdb	0.34	0.05	0.10	52.6
HUPrw	1.39	0.15	0.27	15.4
HUPewb	1.03	0.01	0.04	126.7
HUPlwb	0.73	0.02	0.03	190.4
HUPdb	0.29	0.04	0.02	314.5
FLCrw	0.44	0.16	0.44	7.3
FLCewb	0.97	0.02	0.12	41.4
FLClwb	0.76	0.02	0.14	36.2
FLCdb	0.21	0.09	0.20	22.0
AHArw	0.49	0.09	0.30	13.0
AHAewb	0.07	0.02	0.13	38.8
AHALwb	0.04	0.05	0.16	29.6
AHADb	0.02	0.10	0.11	43.8
DPPrw	0.48	0.11	0.33	11.7
DPPewb	0.89	0.02	0.12	41.9
DPPlwb	0.69	0.02	0.08	65.9
DPPdb	0.21	0.07	0.07	73.9

488

489

490 Table A1: Mean RW, EWB, LWB and DB values for the raw chronologies. Coefficient of variation (CV) and mean inter-series
491 correlation (RBAR) are calculated from the 20-year spline detrended chronologies. n-EPS reflects the number of series needed to
492 attain an EPS value of 0.85 related to the RBAR value (Wilson and Elling 2004).

TASMANIA

RCS - Celery Top

	RCSewb	RCSlwb	RCSdb
RCSrw	0.03	-0.64	0.67
RCSewb		0.22	0.27
RCSlwb			-0.82

MCK - Pencil Pine

	MCKewb	MCKlwb	MCKdb
MCKrw	-0.10	-0.41	0.45
MCKewb		0.57	-0.01
MCKlwb			-0.79

CM - Pencil Pine

	CMewb	CMlwb	CMdb
CMrw	0.01	-0.30	0.43
CMewb		0.68	-0.04
CMlwb			-0.71

MWWTRL - King Billy Pine

	MTewb	MTlwb	MTdb
MTrw	0.31	-0.40	0.62
MTewb		0.21	0.40
MTlwb			-0.76

MRD - King Billy Pine

	MRDewb	MRDlwb	MRDdb
MRDrw	0.18	-0.61	0.65
MRDewb		0.14	0.44
MRDlwb			-0.78

MHP - Huon Pine (high elevation)

	MHPewb	MHPlwb	MHPdb
MHPrw	0.64	-0.19	0.69
MHPewb		0.16	0.67
MHPlwb			-0.56

BUT - Huon Pine (low elevation)

	BUTewb	BUTlwb	BUTdb
BUTrw	-0.20	-0.49	0.31
BUTewb		0.21	0.35
BUTlwb			-0.72

NEW ZEALAND

PKL - Kauri

	PKLewb	PKLlwb	PKLdb
PKLrw	0.14	-0.37	0.54
PKLewb		0.44	0.42
PKLlwb			-0.55

HUP - Kauri

	HUPewb	HUPlwb	HUPdb
HUPrw	-0.02	-0.23	0.30
HUPewb		0.58	0.23
HUPlwb			-0.51

FLC - NZ Cedar

	FLCewb	FLClwb	FLCdb
FLCrw	0.40	-0.47	0.70
FLCewb		0.12	0.58
FLClwb			-0.66

AHA - Silver Pine

	AHAewb	AHALwb	AHAdb
AHArw	0.12	-0.29	0.38
AHAewb		0.48	0.32
AHALwb			-0.58

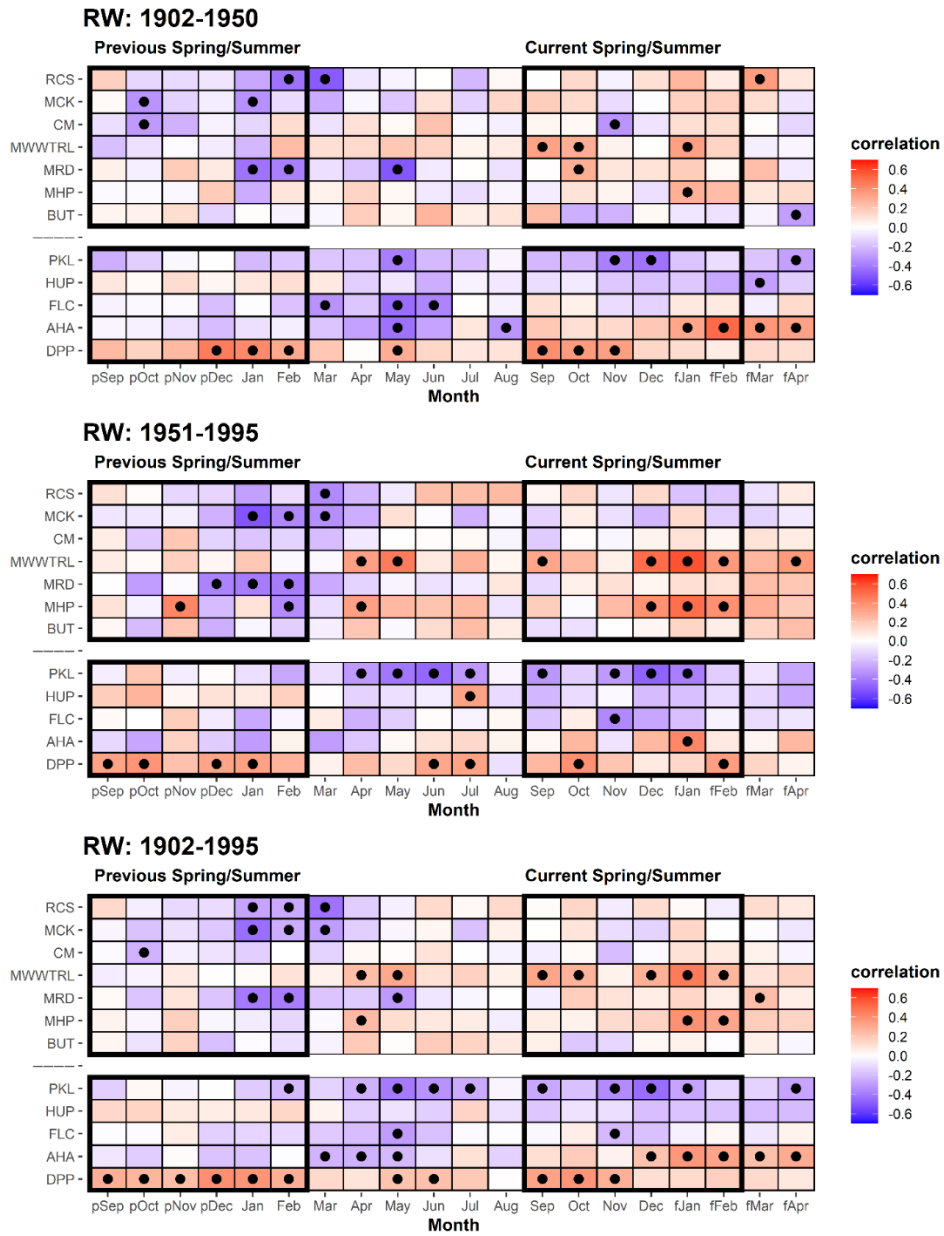
DPP - NZ Pink Pine

	DPPewb	DPPlwb	DPPdb
DPPrw	0.17	-0.25	0.51
DPPewb		0.60	0.60
DPPlwb			-0.20

493

494

495 Table A2: Correlation matrices for each site between the four detrended TR parameter chronologies (1798-1995). Grey shading
496 denotes a significant correlation (95%).

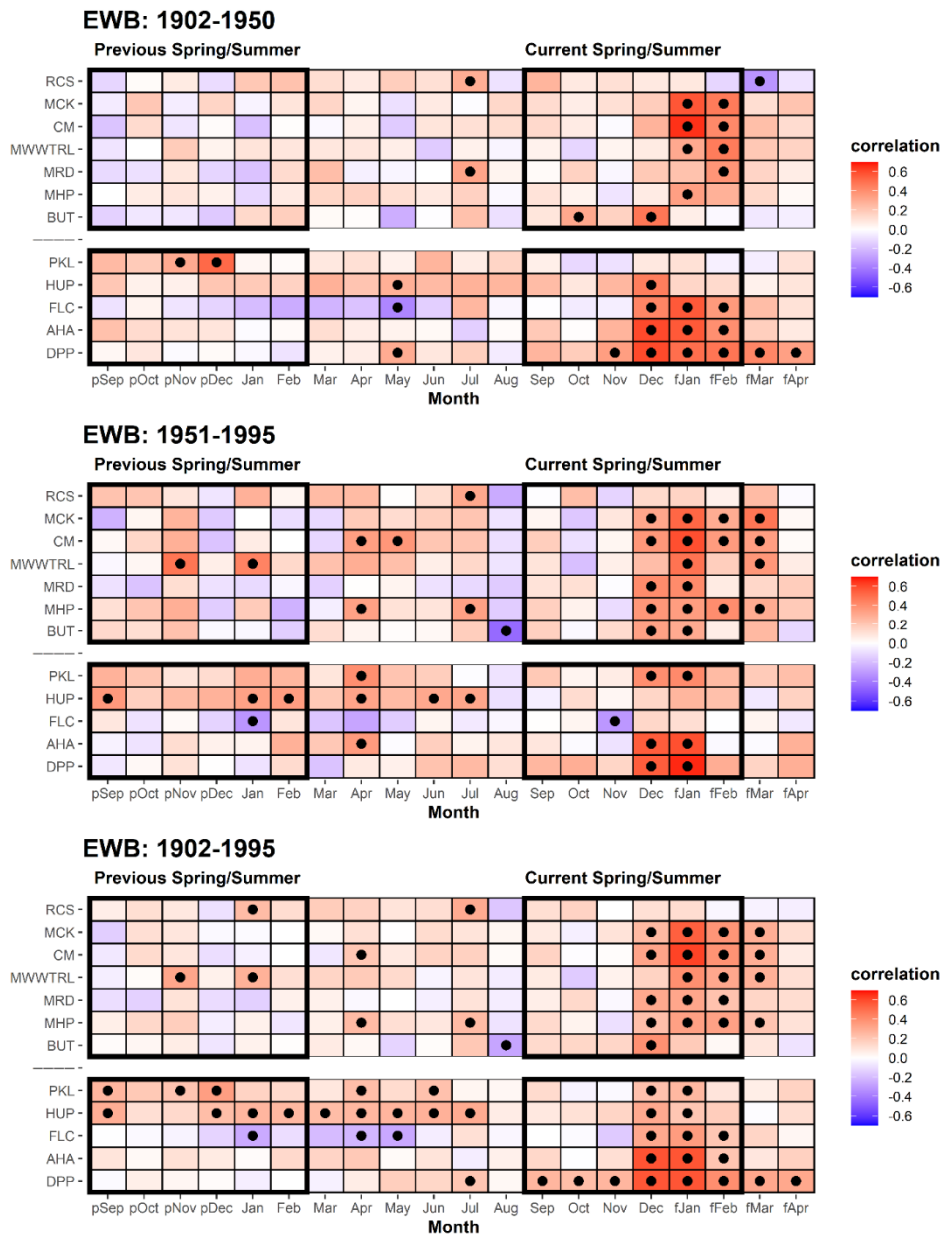


498

499

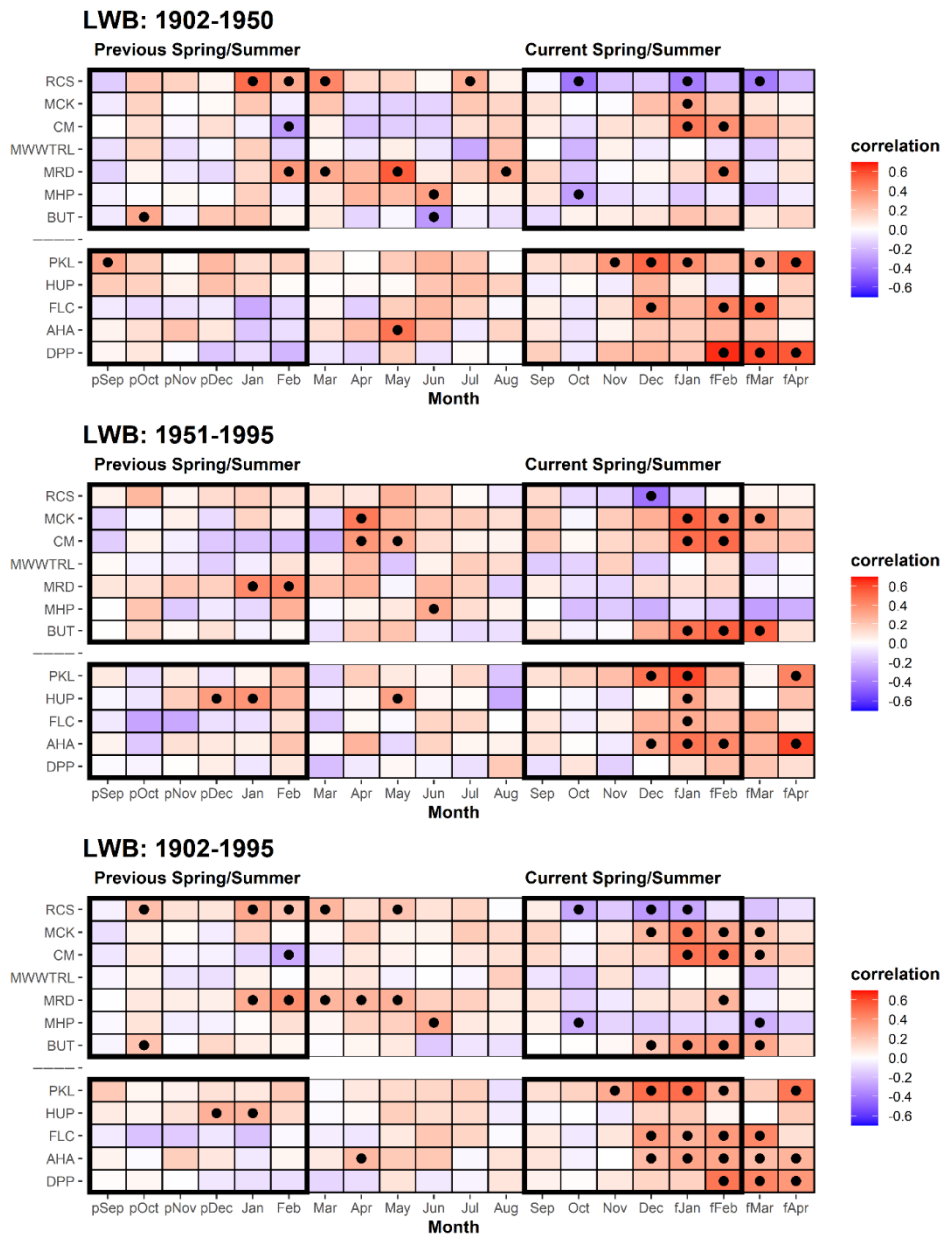
500 **Table A3a: Correlation response function analysis for ring-width with CRU TS temperatures. Analysis was undertaken over the**
 501 **1902-1950, 1951-1995 and 1902-1995 periods. Black dots denoted correlations significant at the 95% C.L.**

502



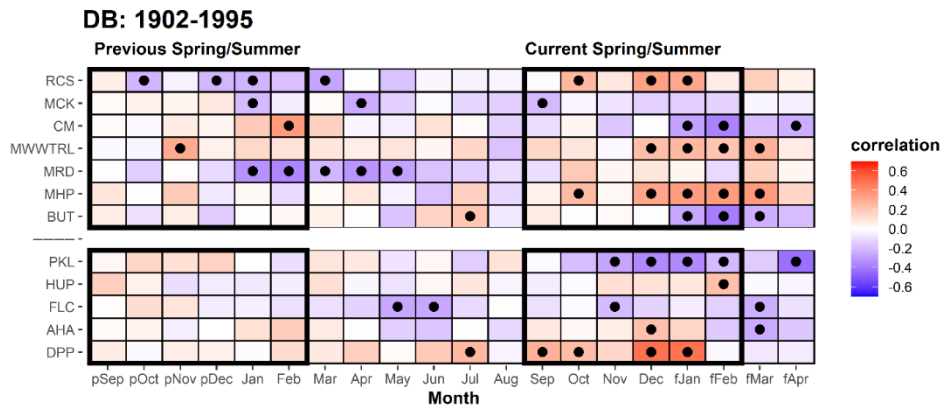
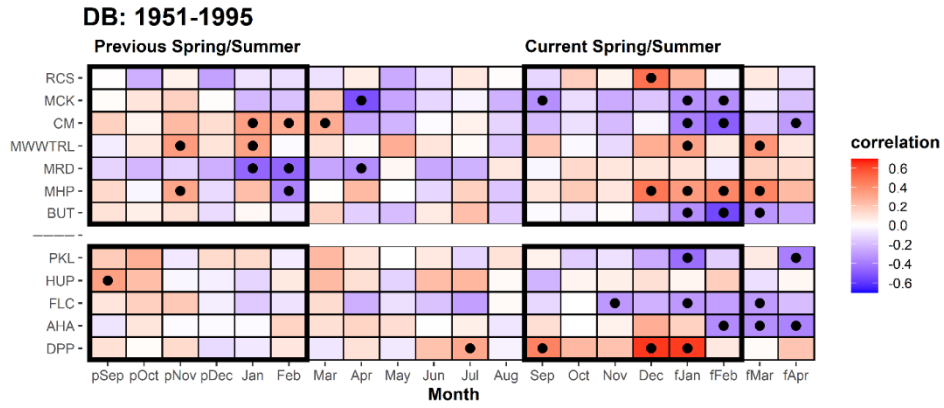
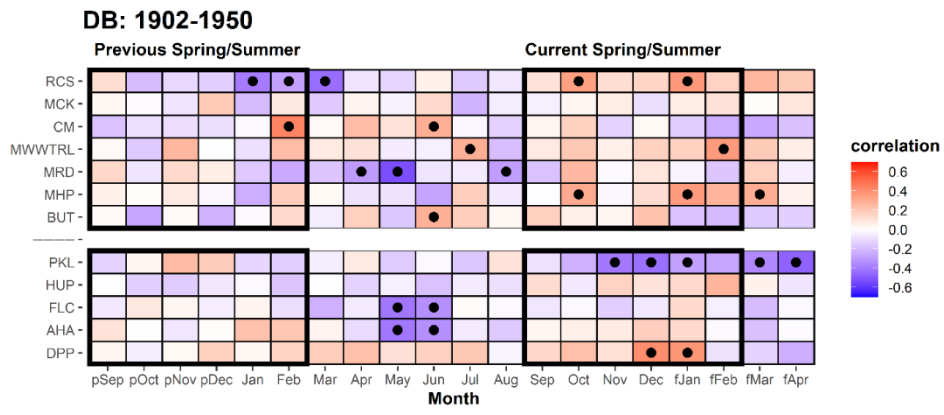
503

504 Table A3b: As 3a but for EWB.



505

506 Table A3c: As 3a but for LWB.

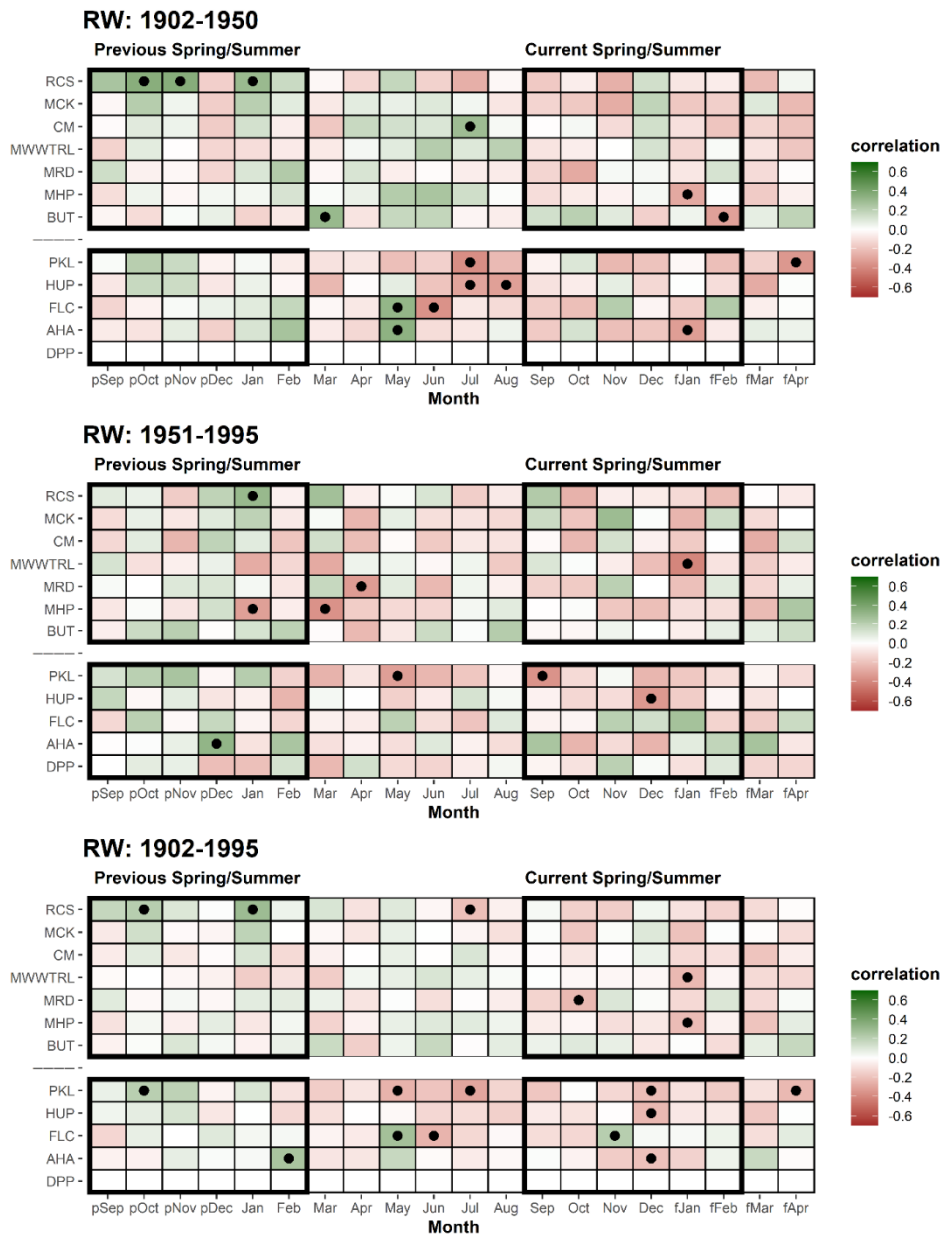


507

508 Table A3d: As 3a but for DB.

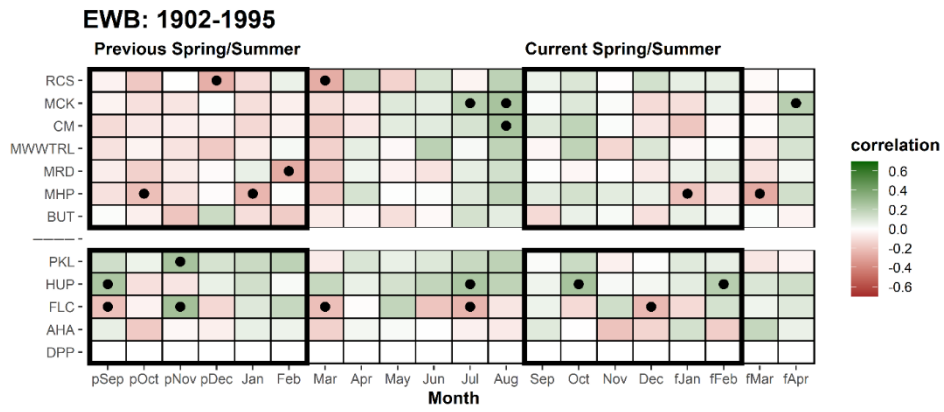
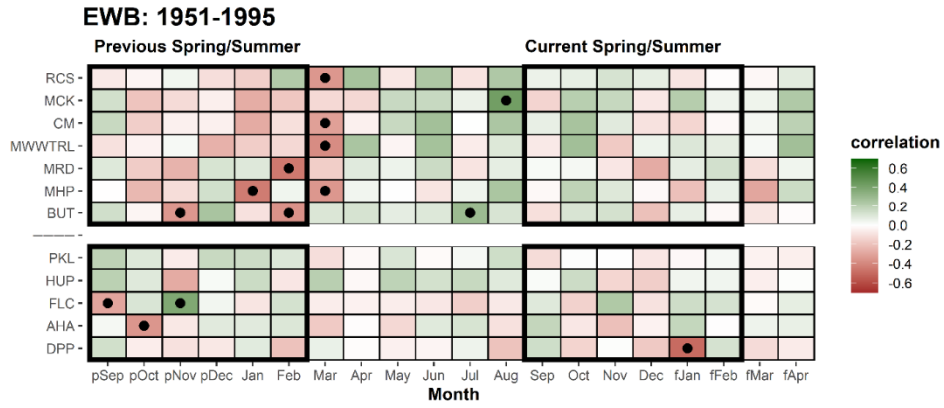
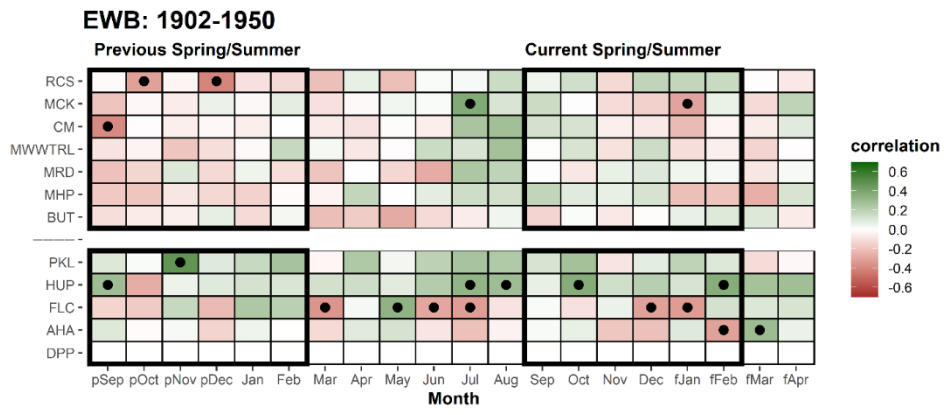
509

510



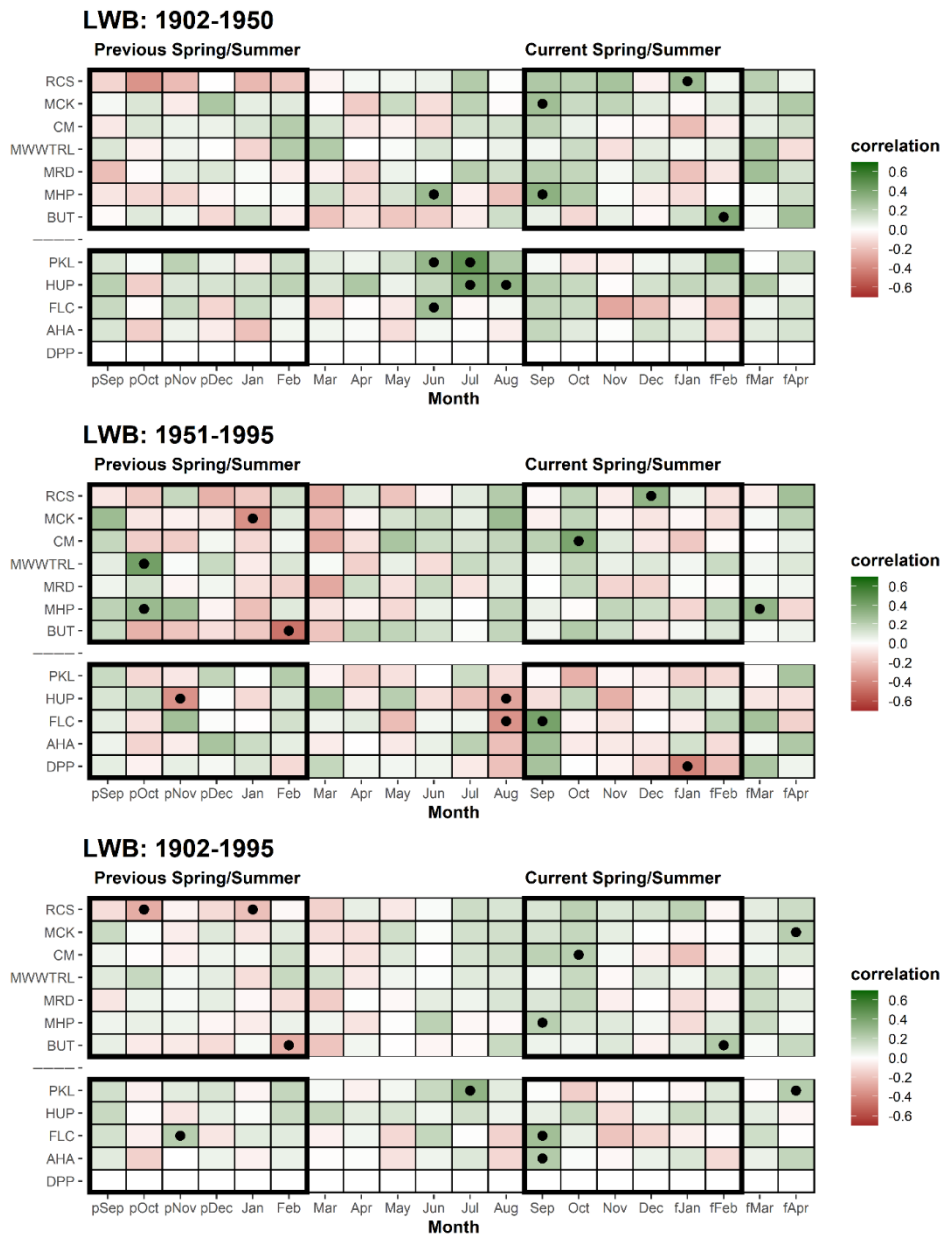
511

512 Table A4a: Correlation response function analysis for ring-width with CRU TS precipitation. Analysis was undertaken over the
 513 1902-1950, 1951-1995 and 1902-1995 periods. Black dots denoted correlations significant at the 95% C.L.



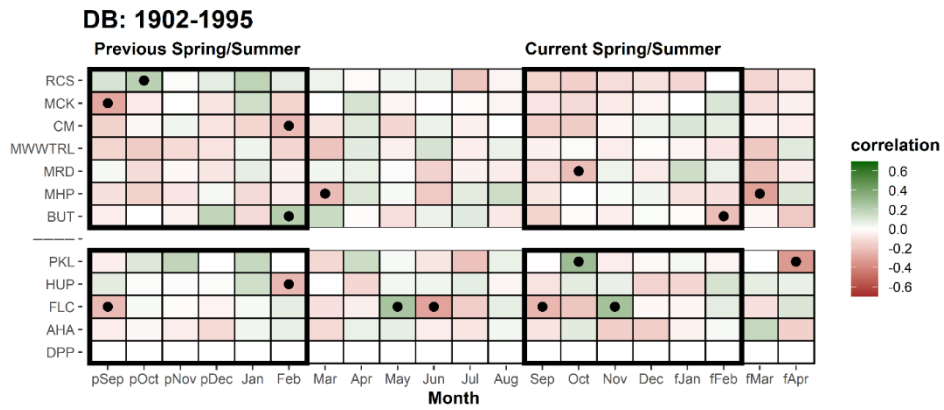
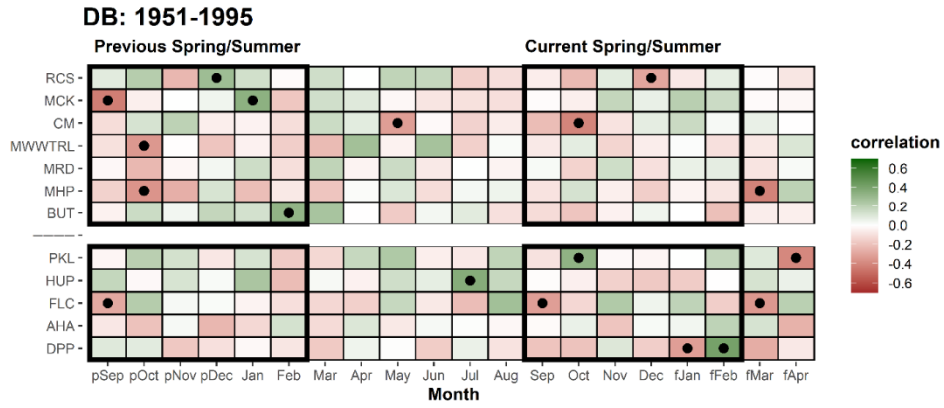
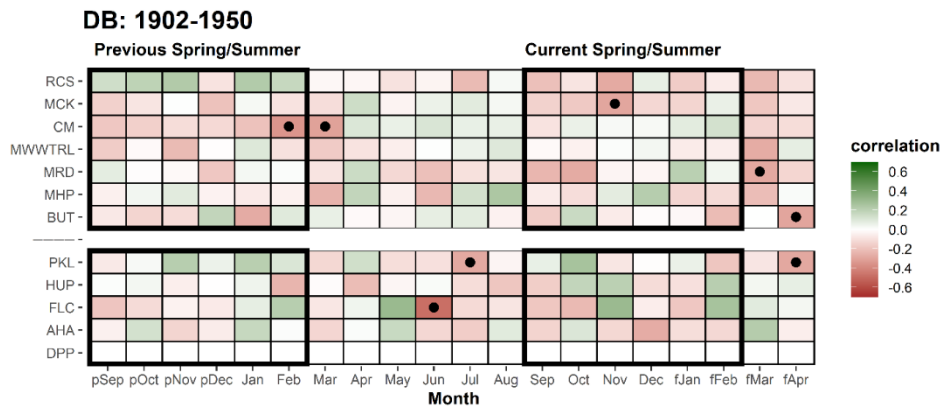
514

515 Table A4b: As 4a but for EWB.



516

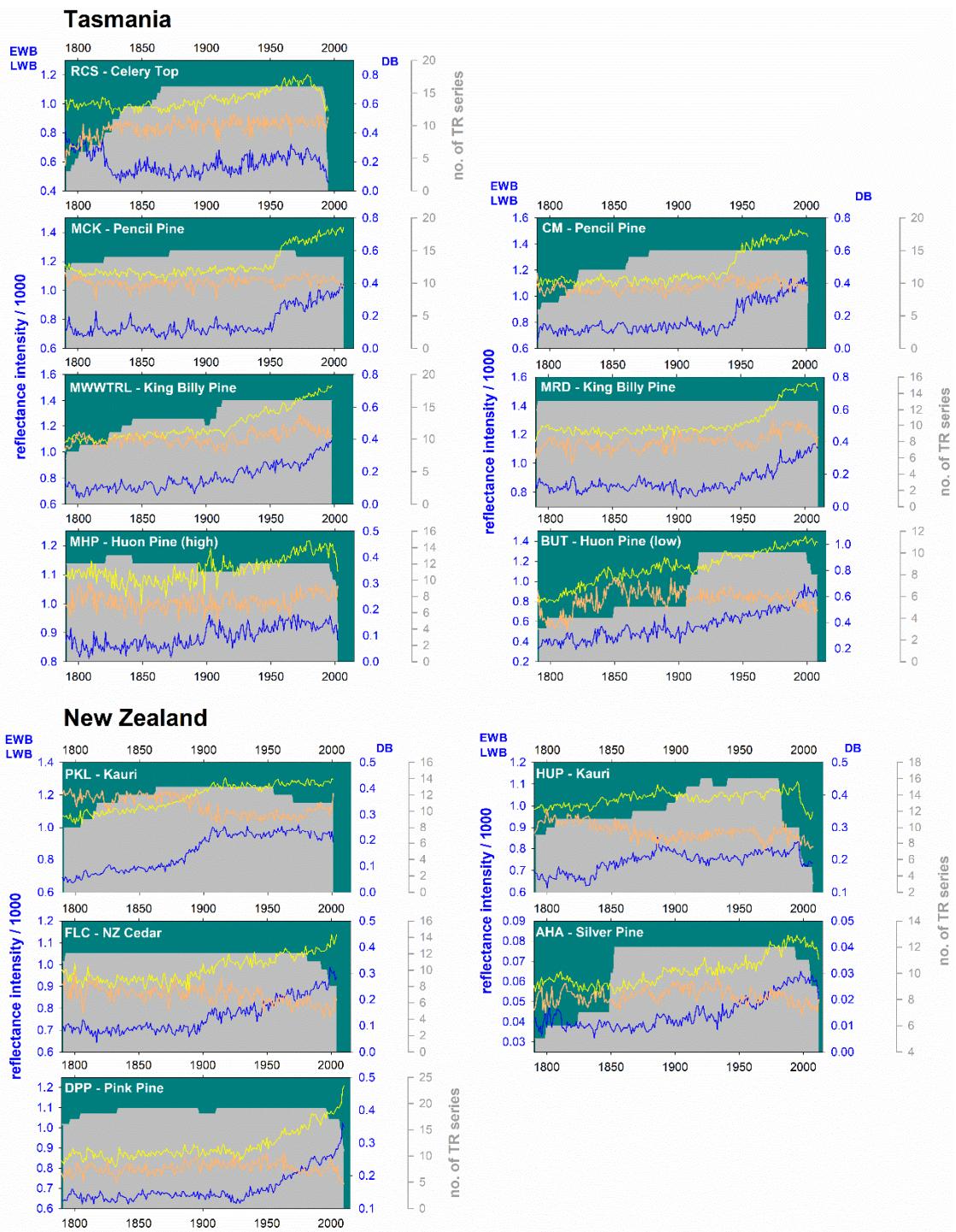
517 Table A4c: As 4a but for LWB.



518

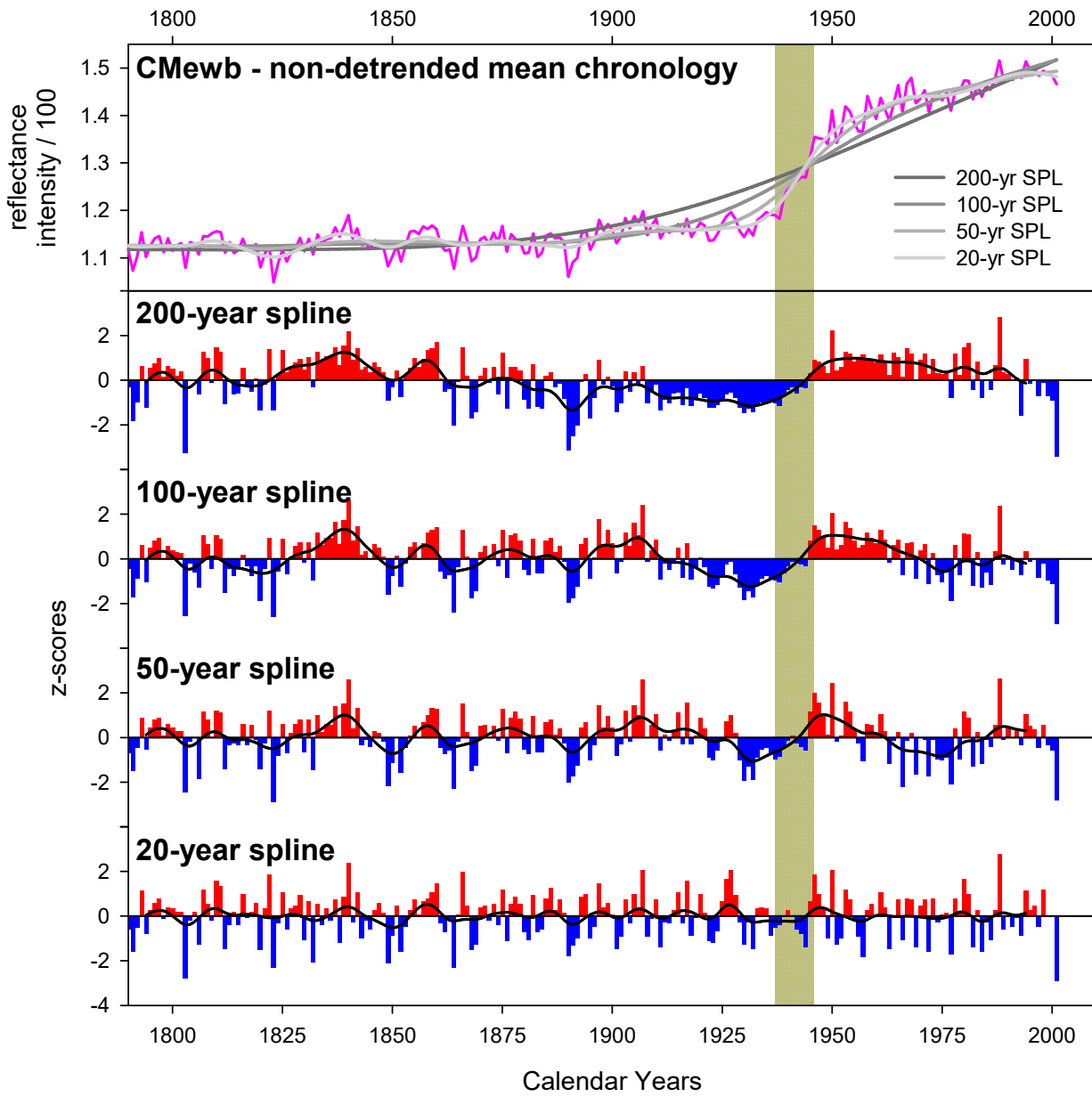
519 Table A4d: As 4a but for DB.

520



521

522 **Figure A1: Plots of raw mean chronologies of EWB (yellow), LWB (blue), DB (orange) and TR series replication (grey shading).**
 523 **The left axis is for EWB and LWB, 1st right axis is DB, while 2nd right axis is series replication.**



525

526

527 Figure A2: Upper panel: raw mean non-detrended EWB chronology for the CM Pencil Pine site. lower panel: represents
528 progressively more flexible spline detrending options. The vertical grey bar denotes the heartwood/sapwood transition period.

529

530

531

532

533 **6 Data availability**

534 All raw data will be archived at the International Tree-Ring Databank on acceptance of the manuscript

535

536 **7 Author contribution**

537 RW: Project conception

538 RW, KA, PB, SB, GB, BB, EC, RD, AF, PK, JP: Sample collection and image acquisition

539 RW, KA, SB, MG: Data generation

540 All: Paper writing, final methodological design, comment and editing

541 **8 Competing interests**

542 The authors declare that they have no conflict of interest

543 **9 Acknowledgements**

544 RW was funded through the University of Melbourne Dyason Fellowship in 2014 to undertake preliminary measurement and
545 analyses for this study. Permission to obtain samples from the Tasmanian sites was provided by Parks and Wildlife
546 Tasmania through several different permits over multiple years. KA was supported by the Australian Research Council
547 grants DP1201040320 and LP12020811 to PB

548 **10 References**

549 Allen, K.J., Cook, E.R., Francey, R.J. and Michael, K., 2001. The climatic response of *Phyllocladus aspleniifolius* (Labill.)
550 Hook. f in Tasmania. *Journal of Biogeography*, 28(3), pp.305-316.

551

552 Allen, K.J., Ogden, J., Buckley, B.M., Cook, E.R. and Baker, P.J., 2011. The potential to reconstruct broadscale climate
553 indices associated with southeast Australian droughts from *Athrotaxis* species, Tasmania. *Climate Dynamics*, 37(9-10),
554 pp.1799-1821.

555

556 Allen, K.J., Lee, G., Ling, F., Allie, S., Willis, M. and Baker, P.J., 2015a. Palaeohydrology in climatological context:
557 developing the case for use of remote predictors in Australian streamflow reconstructions. *Applied Geography*, 64, pp.132-
558 152.

559

560 Allen, K.J., Nichols, S.C., Evans, R., Cook, E.R., Allie, S., Carson, G., Ling, F. and Baker, P.J., 2015b. Preliminary
561 December–January inflow and streamflow reconstructions from tree rings for western Tasmania, southeastern Australia.
562 *Water Resources Research*, 51(7), pp.5487-5503.

563

564 Allen, K.J., Fenwick, P., Palmer, J.G., Nichols, S.C., Cook, E.R., Buckley, B.M. and Baker, P.J., 2017. A 1700-year
565 *Athrotaxis selaginoides* tree-ring width chronology from southeastern Australia. *Dendrochronologia*, 45, pp.90-100.

566

567 Allen, K.J., Cook, E.R., Evans, R., Francey, R., Buckley, B.M., Palmer, J.G., Peterson, M.J. and Baker, P.J., 2018. Lack of
568 cool, not warm, extremes distinguishes late 20th Century climate in 979-year Tasmanian summer temperature
569 reconstruction. *Environmental Research Letters*, 13(3), p.034041.

570

571 Alexander, M.R., Pearl, J.K., Bishop, D.A., Cook, E.R., Anchukaitis, K.J. and Pederson, N., 2019. The potential to
572 strengthen temperature reconstructions in ecoregions with limited tree line using a multispecies approach. *Quaternary*
573 *Research*, 92(2), pp.583-597.

574

575 Altman, J., 2020. Tree-ring-based disturbance reconstruction in interdisciplinary research: Current state and future
576 directions. *Dendrochronologia*, p.125733.

577

578 Arbellay, E., Jarvis, I., Chavardès, R.D., Daniels, L.D. and Stoffel, M., 2018. Tree-ring proxies of larch bud moth
579 defoliation: latewood width and blue intensity are more precise than tree-ring width. *Tree Physiology* 38(8), 1237-1245.

580

581 Babst, F., Poulter, B., Trouet, V., Tan, K., Neuwirth, B., Wilson, R., Carrer, M., Grabner, M., Tegel, W., Levanić, T. and
582 Panayotov, M., 2013. Site-and species-specific responses of forest growth to climate across the European continent. *Global*
583 *Ecology and Biogeography*, 22(6), pp.706-717.

584

585 Babst, F., Wright, W.E., Szejner, P., Wells, L., Belmecheri, S., Monson, R.K., 2016. Blue intensity parameters derived from
586 *Ponderosa* pine tree rings characterize intra-annual density fluctuations and reveal seasonally divergent water limitations.
587 *Trees* 30(4), 1403-1415.

588

589 Björklund, J.A., Gunnarson, B.E., Seftigen, K., Esper, J., Linderholm, H.W., 2014. Blue intensity and density from northern
590 Fennoscandian tree rings, exploring the potential to improve summer temperature reconstructions with earlywood
591 information. *Climate of the Past* 10(2), 877-885.

592

593 Björklund, J., Gunnarson, B.E., Seftigen, K., Zhang, P., Linderholm, H.W., 2015. Using adjusted blue intensity data to attain
594 high-quality summer temperature information: a case study from Central Scandinavia. *The Holocene* 25(3), 547-556.

595

596 Björklund, J., Seftigen, K., Schweingruber, F., Fonti, P., von Arx, G., Bryukhanova, M.V., Cuny, H.E., Carrer, M.,
597 Castagneri, D. and Frank, D.C., 2017. Cell size and wall dimensions drive distinct variability of earlywood and latewood
598 density in Northern Hemisphere conifers. *New Phytologist*, 216(3), pp.728-740.

599

600 Björklund, J., von Arx, G., Nievergelt, D., Wilson, R., Van den Bulcke, J., Günther, B., Loader, N.J., Rydval, M., Fonti, P.,
601 Scharnweber, T. and Andreu-Hayles, L. et al. 2019. Scientific merits and analytical challenges of tree-ring densitometry.
602 *Reviews of Geophysics*, 57(4), pp.1224-1264.

603

604 Björklund, J., Seftigen, K., Fonti, P., Nievergelt, D., von Arx, G., 2020. Dendroclimatic potential of dendroanatomy in
605 temperature-sensitive *Pinus sylvestris*. *Dendrochronologia* 60, 125673.

606

607 Blake, S.A., Palmer, J.G., Björklund, J., Harper, J.B. and Turney, C.S., 2020. Palaeoclimate potential of New Zealand
608 *Manoao colensoi* (silver pine) tree rings using Blue-Intensity (BI). *Dendrochronologia*, 60, p.125664.

609

610 Boswijk, G., Fowler, A.M., Palmer, J.G., Fenwick, P., Hogg, A., Lorrey, A. and Wunder, J., 2014. The late Holocene kauri
611 chronology: assessing the potential of a 4500-year record for palaeoclimate reconstruction. *Quaternary Science Reviews*, 90,
612 pp.128-142.

613

614 Bradley, R.S., 1999. *Paleoclimatology: reconstructing climates of the Quaternary*. Elsevier.

615

616 Briffa, K.R., Osborn, T.J., Schweingruber, F.H., Jones, P.D., Shiyatov, S.G. and Vaganov, E.A., 2002. Tree-ring width and
617 density data around the Northern Hemisphere: Part 1, local and regional climate signals. *The Holocene*, 12(6), pp.737-757.

618

619 Brookhouse, M. and Graham, R., 2016. Application of the minimum blue-intensity technique to a southern-hemisphere
620 conifer. *Tree-Ring Research*, 72(2), pp.103-107.

621

622 Buckley, B.M., Cook, E.R., Peterson, M.J. and Barbetti, M., 1997. A changing temperature response with elevation for
623 *Lagarostrobos franklinii* in Tasmania, Australia. In *Climatic Change at High Elevation Sites* (pp. 245-266). Springer,
624 Dordrecht.

625

626 Buckley, B., Ogden, J., Palmer, J., Fowler, A. and Salinger, J., 2000. Dendroclimatic interpretation of tree-rings in *Agathis*
627 *australis* (kauri). 1. Climate correlation functions and master chronology. *Journal of the Royal Society of New Zealand*,
628 30(3), pp.263-276.

629

630 Buckley, B.M., Hansen, K.G., Griffin, K.L., Schmiege, S., Oelkers, R., D'Arrigo, R.D., Stahle, D.K., Davi, N., Nguyen,
631 T.Q.T., Le, C.N. and Wilson, R.J., 2018. Blue intensity from a tropical conifer's annual rings for climate reconstruction: An
632 ecophysiological perspective. *Dendrochronologia*, 50, pp.10-22.

633

634 Büntgen, U., Krusic, P.J., Verstege, A., Sangüesa-Barreda, G., Wagner, S., Camarero, J.J., Ljungqvist, F.C., Zorita, E.,
635 Oppenheimer, C., Konter, O. and Tegel, W., 2017. New tree-ring evidence from the Pyrenees reveals Western Mediterranean
636 climate variability since medieval times. *Journal of Climate*, 30(14), pp.5295-5318.

637

638 Büntgen, U., Urban, O., Krusic, P.J., Rybníček, M., Kolář, T., Kyncl, T., Ač, A., Koňasová, E., Čáslavský, J., Esper, J. and
639 Wagner, S., 2021. Recent European drought extremes beyond Common Era background variability. *Nature Geoscience*,
640 14(4), pp.190-196.

641

642 Buras, A., 2017. A comment on the expressed population signal. *Dendrochronologia*, 44, pp.130-132.

643

644 Buras, A., Spyt, B., Janecka, K., Kaczka, R., 2018. Divergent growth of Norway spruce on Babia Góra Mountain in the
645 western Carpathians. *Dendrochronologia* 50, 33-43.

646

647 Camarero, J.J., Rozas, V. and Olano, J.M., 2014. Minimum wood density of *Juniperus thurifera* is a robust proxy of spring
648 water availability in a continental Mediterranean climate. *Journal of Biogeography*, 41(6), pp.1105-1114.

649

650 Camarero, J.J., Fernández-Pérez, L., Kirilyanov, A.V., Shestakova, T.A., Knorre, A.A., Kukarskih, V.V. and Voltas, J.,
651 2017. Minimum wood density of conifers portrays changes in early season precipitation at dry and cold Eurasian regions.
652 *Trees*, 31(5), pp.1423-1437.

653

654 Campbell, R., McCarroll, D., Loader, N.J., Grudd, H., Robertson, I., Jalkanen, R., 2007. Blue intensity in *Pinus sylvestris*
655 tree-rings: developing a new palaeoclimate proxy. *The Holocene* 17(6), 821-828.

656
657 Campbell, R., McCarroll, D., Robertson, I., Loader, N.J., Grudd, H., Gunnarson, B., 2011. Blue intensity in *Pinus sylvestris*
658 tree rings: a manual for a new palaeoclimate proxy. *Tree-Ring Research* 67(2), 127-135.
659
660 Cleaveland MK (1986) climatic response of densitometric properties in semiarid site tree rings. *Tree-Ring Bull* 46:13–29
661
662 Cook, E.R. and Peters, K., 1981. The smoothing spline: a new approach to standardizing forest interior tree-ring width series
663 for dendroclimatic studies.
664
665 Cook, E. R. The Decomposition of Tree-Ring Series for Environmental Studies. *Tree-Ring Bulletin* 47 (1987): 37–59.
666
667 Cook, E.R., Briffa, K.R. and Jones, P.D., 1994. Spatial regression methods in dendroclimatology: a review and comparison
668 of two techniques. *International Journal of Climatology*, 14(4), pp.379-402.
669
670 Cook, E.R., Palmer, J.G., Cook, B.I., Hogg, A. and D'Arrigo, R., 2002. A multi-millennial palaeoclimatic resource from
671 *Lagarostrobos colensoi* tree-rings at Oroko Swamp, New Zealand. *Global and Planetary Change*, 33(3-4), pp.209-220.
672
673 Cook, E.R., Buckley, B.M., Palmer, J.G., Fenwick, P., Peterson, M.J., Boswijk, G. and Fowler, A., 2006. Millennia-long
674 tree-ring records from Tasmania and New Zealand: A basis for modelling climate variability and forcing, past, present and
675 future. *Journal of Quaternary Science: Published for the Quaternary Research Association*, 21(7), pp.689-699.
676
677 Cook, E.R. and Pederson, N., 2011. Uncertainty, emergence, and statistics in dendrochronology. In *Dendroclimatology* (pp.
678 77-112). Springer, Dordrecht.
679
680 D'Arrigo, R.D., Buckley, B.M., Cook, E.R. and Wagner, W.S., 1996. Temperature-sensitive tree-ring width chronologies of
681 pink pine (*Halocarpus biformis*) from Stewart Island, New Zealand. *Palaeogeography, Palaeoclimatology, Palaeoecology*,
682 119(3-4), pp.293-300.
683
684 Davi, N.K., Rao, M.P., Wilson, R., Andreu-Hayles, L., Oelkers, R., D'Arrigo, R., Nachin, B., Buckley, B., Pederson, N.,
685 Leland, C. and Suran, B., 2021. Accelerated Recent Warming and Temperature Variability over the Past Eight Centuries in
686 the Central Asian Altai from Blue Intensity in Tree Rings. *Geophysical Research Letters*, p.e2021GL092933.
687
688 Dolgova, E., 2016. June–September temperature reconstruction in the Northern Caucasus based on blue intensity data.
689 *Dendrochronologia* 39, 17-23.

690

691 Drew, D.M., Allen, K., Downes, G.M., Evans, R., Battaglia, M. and Baker, P., 2013. Wood properties in a long-lived conifer
692 reveal strong climate signals where ring-width series do not. *Tree Physiology*, 33(1), pp.37-47.

693

694 Druckenbrod, D.L., Pederson, N., Rentch, J. and Cook, E.R., 2013. A comparison of times series approaches for
695 dendroecological reconstructions of past canopy disturbance events. *Forest ecology and management*, 302, pp.23-33.

696

697 Duncan, R.P., Fenwick, P., Palmer, J.G., McGlone, M.S. and Turney, C.S., 2010. Non-uniform interhemispheric temperature
698 trends over the past 550 years. *Climate Dynamics*, 35(7-8), pp.1429-1438.

699

700 Esper, J., Frank, D.C., Timonen, M., Zorita, E., Wilson, R.J., Luterbacher, J., Holzkämper, S., Fischer, N., Wagner, S.,
701 Nievergelt, D. and Verstege, A., 2012. Orbital forcing of tree-ring data. *Nature Climate Change*, 2(12), pp.862-866.

702

703 Evans R. 1994. Rapid measurement of the transverse dimensions of tracheids in radial wood sections from *Pinus radiata*.
704 *Holzforschung* 48: 168–172.

705

706 Fonti, P., Bryukhanova, M.V., Myglan, V.S., Kirilyanov, A.V., Naumova, O.V. and Vaganov, E.A., 2013. Temperature-
707 induced responses of xylem structure of *Larix sibirica* (Pinaceae) from the Russian Altay. *American journal of botany*,
708 100(7), pp.1332-1343.

709

710 Fowler, A., Palmer, J., Salinger, J. and Ogden, J., 2000. Dendroclimatic interpretation of tree-rings in *Agathis australis*
711 (kauri): 2. Evidence of a significant relationship with ENSO. *Journal of the Royal Society of New Zealand*, 30(3), pp.277-
712 292.

713

714 Fowler, A.M., Boswijk, G., Lorrey, A.M., Gergis, J., Pirie, M., McCloskey, S.P., Palmer, J.G. and Wunder, J., 2012. Multi-
715 centennial tree-ring record of ENSO-related activity in New Zealand. *Nature Climate Change*, 2(3), pp.172-176.

716

717 Fritts, H.C., Smith, D.G., Cardis, J.W. and Budelsky, C.A., 1965. Tree-ring characteristics along a vegetation gradient in
718 northern Arizona. *Ecology*, 46(4), pp.393-401.

719

720 Fritts, H.C. 1976. *Tree Rings and Climate*. London: Academic Press Ltd.

721

722 Fuentes, M., Salo, R., Björklund, J., Seftigen, K., Zhang, P., Gunnarson, B., Aravena, J.C., Linderholm, H.W., 2018. A 970-
723 year-long summer temperature reconstruction from Rogen, west-central Sweden, based on blue intensity from tree rings. *The*
724 *Holocene* 28(2), 254-266.

725

726 Harley, G.L., Heeter, K.J., Maxwell, J.T., Rayback, S.A., Maxwell, R.S., Reinemann, T.E. and H Taylor, A., 2020. Towards
727 broad-scale temperature reconstructions for Eastern North America using blue light intensity from tree rings. *International*
728 *Journal of Climatology*.

729

730 Harris, I.P.D.J., Jones, P.D., Osborn, T.J. and Lister, D.H., 2014. Updated high-resolution grids of monthly climatic
731 observations—the CRU TS3. 10 Dataset. *International journal of climatology*, 34(3), pp.623-642.

732

733 Heeter, K.J., Harley, G.L., Maxwell, J.T., McGee, J.H. and Matheus, T.J., 2020. Late summer temperature variability for the
734 Southern Rocky Mountains (USA) since 1735 CE: applying blue light intensity to low-latitude *Picea engelmannii* Parry ex
735 Engelm. *Climatic Change*, 162(2), pp.965-988.

736

737 Helama, S., Arentoft, B.W., Collin-Haubensak, O., Hyslop, M.D., Brandstrup, C.K., Mäkelä, H.M., Tian, Q. Wilson, R.,
738 2013. Dendroclimatic signals deduced from riparian versus upland forest interior pines in North Karelia, Finland. *Ecological*
739 *Research* 28(6), 1019-1028.

740

741 Kaczka, R.J., Spyt, B., Janecka, K., Beil, I., Büntgen, U., Scharnweber, T., Nievergelt, D., Wilmking, M., 2018. Different
742 maximum latewood density and blue intensity measurements techniques reveal similar results. *Dendrochronologia* 49, 94-
743 101.

744

745 Kaczka, R.J. and Wilson, R., 2021. I-BIND: International Blue Intensity Network Development Working Group.
746 *Dendrochronologia*, p.125859.

747

748 Kienast, F., Schweingruber, F.H., Bräker, O.U. and Schär, E., 1987. Tree-ring studies on conifers along ecological gradients
749 and the potential of single-year analyses. *Canadian Journal of Forest Research*, 17(7), pp.683-696.

750

751 Ljungqvist, F.C., Thejll, P., Björklund, J., Gunnarson, B.E., Piermattei, A., Rydval, M., Seftigen, K., Støve, B. and Büntgen,
752 U., 2020. Assessing non-linearity in European temperature-sensitive tree-ring data. *Dendrochronologia*, 59, p.125652.

753

754 Loader, N.J., Santillo, P.M., Woodman-Ralph, J.P., Rolfe, J.E., Hall, M.A., Gagen, M., Robertson, I., Wilson, R., Froyd,
755 C.A. and McCarroll, D., 2008. Multiple stable isotopes from oak trees in southwestern Scotland and the potential for stable
756 isotope dendroclimatology in maritime climatic regions. *Chemical Geology*, 252(1-2), pp.62-71.
757

758 Loader, N.J., Young, G.H., McCarroll, D., Davies, D., Miles, D. and Bronk Ramsey, C., 2020. Summer precipitation for the
759 England and Wales region, 1201–2000 CE, from stable oxygen isotopes in oak tree rings. *Journal of Quaternary Science*.
760

761 Lorimer, C.G. and Frelich, L.E., 1989. A methodology for estimating canopy disturbance frequency and intensity in dense
762 temperate forests. *Canadian Journal of Forest Research*, 19(5), pp.651-663.
763

764 McCarroll, D., Pettigrew, E., Luckman, A., Guibal, F. and Edouard, J.L., 2002. Blue reflectance provides a surrogate for
765 latewood density of high-latitude pine tree rings. *Arctic, Antarctic, and Alpine Research*, 34(4), pp.450-453.
766

767 McCarroll, D. and Loader, N.J., 2004. Stable isotopes in tree rings. *Quaternary Science Reviews*, 23(7-8), pp.771-801.
768

769 Neukom, R., Gergis, J., Karoly, D.J., Wanner, H., Curran, M., Elbert, J., González-Rouco, F., Linsley, B.K., Moy, A.D.,
770 Mundo, I. and Raible, C.C., 2014. Inter-hemispheric temperature variability over the past millennium. *Nature Climate*
771 *Change*, 4(5), pp.362-367.
772

773 O'Donnell, A.J., Allen, K.J., Evans, R.M., Cook, E.R., Trouet, V. and Baker, P.J., 2016. Wood density provides new
774 opportunities for reconstructing past temperature variability from southeastern Australian trees. *Global and Planetary*
775 *Change*, 141, pp.1-11.
776

777 Palmer, J.G. and Xiong, L., 2004. New Zealand climate over the last 500 years reconstructed from *Libocedrus bidwillii*
778 *Hook. f.* tree-ring chronologies. *The Holocene*, 14(2), pp.282-289.
779

780 Panyushkina, I.P., Hughes, M.K., Vaganov, E.A. and Munro, M.A., 2003. Summer temperature in northeastern Siberia since
781 1642 reconstructed from tracheid dimensions and cell numbers of *Larix cajanderi*. *Canadian Journal of Forest Research*,
782 33(10), pp.1905-1914.
783

784 Prendin, A.L., Petit, G., Carrer, M., Fonti, P., Björklund, J. and von Arx, G., 2017. New research perspectives from a novel
785 approach to quantify tracheid wall thickness. *Tree Physiology*, 37(7), pp.976-983.
786

787 Reid, E. and Wilson, R., 2020. Delta Blue Intensity vs. Maximum Density: A Case Study using *Pinus uncinata* in the
788 Pyrenees. *Dendrochronologia*, p.125706.
789

790 Rohde R, Muller RA, Jacobsen R et al. (2013) A new estimate of the average earth surface land temperature spanning 1753
791 to 2011. *Geoinformatics & Geostatistics: An Overview 1: 1*. doi: 10.4172/2327-4581.1000101.
792

793 Rydval, M., Larsson, L.Å., McGlynn, L., Gunnarson, B.E., Loader, N.J., Young, G.H., Wilson, R., 2014. Blue intensity for
794 dendroclimatology: should we have the blues? Experiments from Scotland. *Dendrochronologia* 32(3), 191-204.
795

796 Rydval, M., Druckenbrod, D., Anchukaitis, K.J. and Wilson, R., 2016. Detection and removal of disturbance trends in tree-
797 ring series for dendroclimatology. *Canadian Journal of Forest Research*, 46(3), pp.387-401.
798

799 Rydval, M., Loader, N.J., Gunnarson, B.E., Druckenbrod, D.L., Linderholm, H.W., Moreton, S.G., Wood, C.V. and Wilson,
800 R., 2017. Reconstructing 800 years of summer temperatures in Scotland from tree rings. *Climate Dynamics*, 49(9-10),
801 pp.2951-2974.
802

803 Rydval, M., Druckenbrod, D.L., Svoboda, M., Trotsiuk, V., Janda, P., Mikoláš, M., Čada, V., Bače, R., Teodosiu, M.,
804 Wilson, R., 2018. Influence of sampling and disturbance history on climatic sensitivity of temperature-limited conifers. *The*
805 *Holocene* 28(10), 1574-1587.
806

807 Seftigen, K., Fuentes, M., Ljungqvist, F.C. and Björklund, J., 2020. Using Blue Intensity from drought-sensitive *Pinus*
808 *sylvestris* in Fennoscandia to improve reconstruction of past hydroclimate variability. *Climate Dynamics*, pp.1-16.
809

810 St. George, S., 2014. An overview of tree-ring width records across the Northern Hemisphere. *Quaternary Science Reviews*,
811 95, pp.132-150.
812

813 Trotsiuk, V., Pederson, N., Druckenbrod, D.L., Orwig, D.A., Bishop, D.A., Barker-Plotkin, A., Fraver, S. and Martin-Benito,
814 D., 2018. Testing the efficacy of tree-ring methods for detecting past disturbances. *Forest Ecology and Management*, 425,
815 pp.59-67.
816

817 Visser, H. and Molenaar, J., 1988. Kalman filter analysis in dendroclimatology. *Biometrics*, pp.929-940.
818

819 von Arx, G., Crivellaro, A., Prendin, A.L., Čufar, K. and Carrer, M., 2016. Quantitative wood anatomy—practical
820 guidelines. *Frontiers in plant science*, 7, p.781.

821
822 Wang, L., Payette, S. and Bégoin, Y., 2002. Relationships between anatomical and densitometric characteristics of black
823 spruce and summer temperature at tree line in northern Quebec. *Canadian Journal of Forest Research*, 32(3), pp.477-486.
824
825 Wigley, T.M., Briffa, K.R. and Jones, P.D., 1984. On the average value of correlated time series, with applications in
826 dendroclimatology and hydrometeorology. *Journal of Applied Meteorology and Climatology*, 23(2), pp.201-213.
827
828 Wiles, G.C., Charlton, J., Wilson, R.J., D'Arrigo, R.D., Buma, B., Krapek, J., Gaglioti, B.V., Wiesenberg, N., Oelkers, R.,
829 2019. Yellow-cedar blue intensity tree-ring chronologies as records of climate in Juneau, Alaska, USA. *Canadian Journal of*
830 *Forest Research* 49(12), 1483-1492.
831
832 Wilmking, M., van der Maaten-Theunissen, M., van der Maaten, E., Scharnweber, T., Buras, A., Biermann, C., Gurskaya,
833 M., Hallinger, M., Lange, J., Shetti, R. and Smiljanic, M., 2020. Global assessment of relationships between climate and tree
834 growth. *Global Change Biology*, 26(6), pp.3212-3220.
835
836 Wilson, R.J. and Hopfmueller, M., 2001. Dendrochronological investigations of Norway spruce along an elevational transect
837 in the Bavarian Forest, Germany. *Dendrochronologia*, 19(1), pp.67-79.
838
839 Wilson, R.J. and Luckman, B.H., 2003. Dendroclimatic reconstruction of maximum summer temperatures from upper
840 treeline sites in Interior British Columbia, Canada. *The Holocene*, 13(6), pp.851-861.
841
842 Wilson, R. and Elling, W., 2004. Temporal instability in tree-growth/climate response in the Lower Bavarian Forest region:
843 implications for dendroclimatic reconstruction. *Trees*, 18(1), pp.19-28.
844
845 Wilson, R.J.S, Rao, R., Rydval, M., Wood, C., Larsson, L.-A., Luckman, B.H. 2014. Blue Intensity for Dendroclimatology:
846 The BC Blues: A Case Study from British Columbia Canada. *The Holocene* 24 (11), 1428-1438.
847
848 Wilson, R., Wilson, D., Rydval, M., Crone, A., Büntgen, U., Clark, S., Ehmer, J., Forbes, E., Fuentes, M., Gunnarson, B.E.,
849 Linderholm, H., Nicolussi, K., Wood, C., Mills, C. 2017a. Facilitating tree-ring dating of historic conifer timbers using Blue
850 Intensity. *Journal of Archaeological Science* 78, 99-111.
851
852 Wilson, R., D'Arrigo, R., Andreu-Hayles, L., Oelkers, R., Wiles, G., Anchukaitis, K., Davi, N., 2017b. Experiments based on
853 blue intensity for reconstructing North Pacific temperatures along the Gulf of Alaska. *Climate of the Past* 13(8), 1007-1022.
854

855 Wilson, R., Anchukaitis, K., Andreu-Hayles, L., Cook, E., D'Arrigo, R., Davi, N., Haberbauer, L., Krusic, P., Luckman, B.,
856 Morimoto, D., Oelkers, R., 2019. Improved dendroclimatic calibration using blue intensity in the southern Yukon. *The*
857 *Holocene* 29(11), 1817-1830.
858
859 Xiong, L., Okada, N., Fujiwara, T., Ohta, S. and Palmer, J.G., 1998. Chronology development and climate response analysis
860 of different New Zealand pink pine (*Halocarpus biformis*) tree-ring parameters. *Canadian Journal of Forest Research*, 28(4),
861 pp.566-573.
862
863 Yasue, K., Funada, R., Kobayashi, O. and Ohtani, J., 2000. The effects of tracheid dimensions on variations in maximum
864 density of *Picea glehnii* and relationships to climatic factors. *Trees*, 14(4), pp.223-229.
865
866 Young, G.H., Loader, N.J., McCarroll, D., Bale, R.J., Demmler, J.C., Miles, D., Nayling, N.T., Rinne, K.T., Robertson, I.,
867 Watts, C. and Whitney, M., 2015. Oxygen stable isotope ratios from British oak tree-rings provide a strong and consistent
868 record of past changes in summer rainfall. *Climate Dynamics*, 45(11-12), pp.3609-3622.